SIMULATION AND STATISTICAL MODELING APPROACHES TO INVESTIGATE DOMINANT CONTROLS ON HYDROLOGIC REGIME TRANSFORMATIONS FOLLOWING EASTERN HEMLOCK MORTALITY

A Thesis

Presented to the Faculty of the Graduate School

of Cornell University

In Partial Fulfillment of the Requirements for the Degree of

Master of Science

by

Kanishka Singh

May 2019

ABSTRACT

Ecohydrologic controls on the critical zone are strongly influenced by Eastern hemlock (*Tsuga canadensis*), a foundation tree species established throughout much of Eastern North America. Eastern hemlock populations are currently threatened by the hemlock woolly adelgid (*Adelges tsugae*), an invasive insect. Hemlock woolly adelgid populations have been expanding rapidly throughout the native Eastern hemlock range. Given the complex relationships between canopy interception, unsaturated and saturated groundwater storage, and root water uptake, it is not immediately clear how Eastern hemlock loss will affect the hydrologic cycle. This research presents a review of past studies on this theme, and then investigates the hydrologic impact of Eastern hemlock mortality across a regional sample of catchments utilizing simulation and statistical modeling approaches. Modeling outcomes suggest that Eastern hemlock mortality will augment flooding potential. Finally, summaries of future studies examining Eastern hemlock plant hydraulics and control of fluvial flooding are presented.

BIOGRAPHICAL SKETCH

It is the year 2019. Kanishka Singh is a human inhabitant of planet Earth who loves science, particularly the science of plant-water interactions. Thank you, reader, for your interest in his work. Pleasant journeys and happy landings.

For S.B. and the pursuit of a better understanding of our astonishing planet.

ACKNOWLEDGMENTS

I would like to acknowledge my committee for their consistent guidance. I thank Dr. James P. Lassoie for his kindness and inspiration, his tireless review of my work, and his wonderful friendship. With his encouragement and approval, I have been able to pursue science as a career, and I will forever be grateful for him. I thank Dr. Todd Walter for his enthusiasm, his patience, and for generously accepting me to his lab and introducing me to the incredible world of hydrologic engineering. I am thankful for all I have learned from him. I thank Dr. Bill Philpot, whose class I always left with a renewed appreciation for the beauty of our natural world, and who set this tone early for all the courses I took since.

I would also like to express gratitude for my friends and colleagues at the Soil and Water Lab. I look forward to working with these brilliant people throughout my graduate school years and beyond. A special thanks to my collaborator James Knighton for being a great mentor and friend.

Finally, I am privileged to have the warmth and support of my mother, father, sister, and my partner Ettie.

TABLE OF CONTENTS

LIST OF FIGURES

LIST OF TABLES

CHAPTER 1

BACKGROUND AND OBJECTIVES

Our planet's freshwater, while a modicum of its total water supply, abounds around us. It courses across an inconstant topography as rushing headwater streams and sinuous lowland rivers, channeling through forests and shrubland, spilling into wetlands, draining to estuaries, converging in lakes and subterranean reservoirs. Through its tortuous journey, water delivers itself in service of biotic form and function at every scale, from the physiological activity that enables plants to survive and grow, to great watersheds that support prodigious biodiversity and supply human use. Their seeming ubiquity notwithstanding, our water resources are stressed to assuage drinking water and sanitation demands, and human modification of hydrologic processes frequently damages water-dependent ecosystems (Wood et al., 2008a; Loucks et al., 2017, p. 1-2). On the other hand, precipitation responses to the rising planetary surface temperature are projected to drive increases in the frequency and intensity of fluvial flooding events, compounding water pollution and aquatic habitat destruction, devastating infrastructure, and displacing human communities (Willner et al., 2018).

The indivisibility of freshwater conditions from surrounding vegetation characteristics and the many physical interrelationships that maintain the integrity of these two intrinsic parts of catchment areas can often confound water resource management and research (Hornberger et al., 2014, p. 240-251; Wood et al., 2008a). At the outset of global climate research, vegetation was not perceived as a significant regulator of the hydrologic and energy cycles, which, even in their terrestrial manifestations, were believed to be controlled primarily by ocean-atmosphere processes (Gordon and Huxman, 2008). Research has since reversed this perspective, and it is

now established that land surface features exert a critical influence on key hydrologic processes such as evaporation and runoff. Even individual plant species can exercise an inordinate control on forest transpiration and interception, the removal of which from a forested ecosystem may profoundly transform the local water cycle (Bosch and Hewlett, 1982; Swank et al., 1988; Pataki and Oren, 2003; Ewers et al., 2005).

While in the case of ocean-atmosphere relations, boundary conditions can be set in accordance with fluid mechanics and the classical laws of thermodynamics, the boundary conditions of terrestrial hydrologic processes are determined by more dynamic biological processes. Further, land surface features and the atmosphere exert a reciprocating influence; that is, vegetation may determine climatic attributes, and the climate may regulate vegetation characteristics (Eagleson, 2002). Indeed, research indicates that hydrologic phenomena at the land surface are directed by a confluence of local climate, vegetation, and soil characteristics (Rodriquez-Iturbe et al., 2001; Lemordant et al., 2018).

Hence, the quality and quantity of water available in a watershed is a function of the cumulative influences of factors that threaten land surface features and transform the processes that link terrestrial ecosystems with the hydrologic cycle. One such process, of natural interest to forest and water resource managers, is the relationship between vegetation die-off and the water cycle. While the ecohydrologic consequences of forest harvest have been widely studied, research examining changes in water budgets following other forms of disturbance, such as invasive insect outbreaks, is relatively scarce (Adams et al., 2012; Brantley et al., 2014). Evaluations of the potential of infestation-triggered vegetation decline to alter catchment water availability are increasingly pertinent as warmer temperatures drive both extreme precipitation and tree vulnerability, all the while allowing for the expansion of invasive insect ranges

(McDowell et al., 2008; Raffa et al., 2008; Allen et al., 2010; Frei et al., 2015; Huang et al., 2017). Thus, the ongoing proliferation of the hemlock woolly adelgid (*Adelges tsugae*) (HWA), a sap-feeding insect, and the ensuing decline of Eastern hemlock (*Tsuga canadensis*) (EH), a foundation conifer species that has been found to regulate ecological and hydrologic conditions in its proximity (Jenkins et al., 1999; Lovett et al., 2004; Kim et al., 2017) is of immediate relevance.

EH performs a variety of vital ecosystem services, such as regulating rates of soil nitrogen (N) mineralization, nitrification, and N turnover (Jenkins et al., 1999), and modulating local water cycling and microclimatic conditions by transpiring year-round and providing denser shade relative to hardwood species (Ford and Vose, 2007; Sidehurst et al., 2010). HWA infestations progress rapidly and have contributed to extensive EH decline throughout Eastern U.S., catalyzing a cascade of hydrologic and biogeochemical dynamics that may modify terrestrial and aquatic ecosystems alike by altering water balance components, flow partitioning patterns, local soil conditions, streamflow regimes, nutrient cycling, and potentially surface water pollution from increased nutrient input (Jenkins et al., 1999; Yorks et al., 2000; Stadler et al., 2005; Cessna and Nielsen, 2012).

Arguably, streamflow regime transformations and nutrient pollution risk driven by EH mortality are both mediated by hydrologic pathways such as surface runoff. Overland runoff is, in turn, determined by interactions between EH condition and water cycle components such as streamflow and evapotranspiration (ET) partitioning, soil-water availability, infiltration, and catchment storage. Much of the limited existing research literature assessing the hydrologic outcomes of HWA outbreak is plot-scale (Daley et al., 2007; Ford and Vose, 2007; Hadley et al., 2008; Lustenhouwer et al., 2012; Domec et al., 2013), and consequently findings produced by

these studies regarding the relevant hydrologic mechanisms may lack generalizability at the catchment or regional levels. In order to support the expansion of the spatial scope of this topic, the present research investigates hydrologic repercussions of EH mortality at regional scale, utilizing a multi-state sample of catchments spanning the Northeastern and Southeastern U.S., across the native EH range. Further, through a combination of statistical and simulation modeling approaches, physical dynamics responsible for water cycle modulations relevant at the regional scale are identified. The broad objectives of this study are:

1. Surveying salient literature to deliver a synthesis of hydrologic trends and mechanistic processes following EH mortality as well as ecological succession at tree, plot, and catchment scales (Chapter 2).
2. Conducting a multi-state study of hydrologic regime changes associated with EH presence and condition through the application of computer simulation and statistical modeling to assess the validity of previous research findings at a broader scale (Chapter 3).
3. Proposing a series of future studies that improve the precision of the work presented here in exploring EH hydraulic control of flooding potential (Chapter 4).

CHAPTER 2

REVIEW OF RELEVANT THEORY AND PREVIOUS RESEARCH

2.1 Introduction

Studies exploring catchment scale water balance changes following deforestation and afforestation find that stream discharge tends to increase in the case of the former and decline in the latter, but the seasonal pattern and total extent of this alteration remains unpredictable (Swank et al., 1988). The comparatively scarce literature examining the hydrological consequence of EH mortality specifically achieves less consensus, arriving at varying results and predictions regarding ET and streamflow regime alterations. Chapter 3 of this thesis expands the spatial scope of this line of inquiry to assess the regional generalizability of previous, smaller scale research. As forest and water resource managers must be able to both anticipate the direction of hydrologic shifts and understand their primary driving processes to most effectively mitigate the consequences of HWA infestation, this work further browses mechanistic explanations. To frame an informed discussion of the findings presented later in Chapter 3, this chapter provides a review of relevant theory, followed by a survey of past research that follows the ecohydrologic consequences of EH mortality from the tree to the catchment-scale.

2.2 Fundamentals of Relevant Ecohydrological Processes

A foundational concept in the science of hydrology is the hydrologic cycle, or the perpetual, global movement of water between the atmosphere, land surfaces, and the oceans in gaseous, liquid, and solid forms. This cycling is driven primarily by solar radiation and gravity; incident radiant energy on the water surface promotes its vaporization into the atmosphere and precipitation occurs as gravity replaces this water vapor lost from the Earth's surface (Hornberger et al., 2014, p. 7).

Precipitation falling on the terrestrial surface is redistributed among some subset of basic hydrologic processes: a fraction of bulk precipitation is intercepted by vegetation and subsequently evaporates given sufficient energy input; the remainder falls to the soil either immediately or following a delay within the canopy, a process referred to as throughfall; of the water that arrives at the soil, some is returned to the atmosphere by way of plant uptake, or given a vapor gradient between the surface and the air and sufficient energy input, by transpiration and evaporation; the remaining balance either flows directly across the soil surface or across some deeper soil horizon as runoff to discharge at nearby surface water bodies, or alternatively infiltrates deeper into the soil to supply groundwater reserves; finally, a volume of the groundwater storage supplements neighboring surface water as baseflow (Hibbert and Troendle, 1988; Hornberger et al., 2014, p. 7).

In accounting for the flow of water within a given geographic area, hydrologists employ the law of conservation of mass and express the processes constituting the hydrologic cycle quantitatively as components of a water balance equation. Most often, this geographic area is a watershed (also termed a catchment or drainage basin), a hydrologic unit of analysis defined as

the geographic extent of topographic features that deliver all available water to any given cross-section of a stream. Therefore, a different catchment area can be delineated for any point of flow convergence and its borders are referred to as a divide (Dingman, 2002, p. 10; Hornberger et al., 2014, p. 14).

The water balance equation for any catchment measures the time rate of change of water within a storage medium (which in this case may be the catchment itself), given water inflow and outflow rates (Hornberger et al., 2014, p. 15-16). Integrating the various processes that constitute the water cycle, the equation can be expressed for any discrete time period as:

$$\Delta S = P + G_{in} - Q - ET - G_{out} \quad (1)$$

Where ΔS is the change in water storage within the catchment for a given timestep, P is the flux of solid and liquid precipitation, Q is the flux of stream outflow or discharge, ET is evapotranspiration flux as vapor, and G_{in} and G_{out} are groundwater inflows and outflow fluxes, respectively (Dingman, 2002, p. 12). Evaporation and transpiration fluxes have traditionally been combined as ET, as it is not methodologically easy to measure the two processes separately, although modern approaches that capitalize on the isotopic enrichment differential between water evaporated from soil and transpired from leaves render the distinction possible to some extent (Bond et al., 2008; Sprenger et al., 2016).

Water budgets calculations usually neglect G_{in}, and G_{out} at the regional scale. Further, over several years of analysis, assuming no substantial climatic, geologic, or anthropogenic perturbations, change in storage within a watershed is assumed to be insignificant as well (Dingman, 2002, p. 12). Considering that the purpose of Chapter 3 is to identify coarse

hydrologic trends and their relationship with EH condition using long-term data, the terms G_{in}, G_{out}, and ΔS have been omitted from the annual water budget.

It is necessary here to differentiate between reference-crop evapotranspiration or potential evapotranspiration (PET) and actual evapotranspiration (AET). The former was initially conceptualized as a measure of the rate of ET in a uniformly and totally vegetated area with a boundless supply of water and immune to any advection or heat-storage phenomena (Dingman, 2002, p. 308-311). Notwithstanding an infinite water supply, surface characteristics do indeed play a great role in determination of vapor flux, and cannot be ignored. Hence, the concept is typically used to describe transpiration rates from a short crop of uniform height that completely shades the ground (thereby minimizing the evaporation component).

Despite its assumptions of ideal conditions, PET measurements for any location are often used as indices of the role of ambient local climatic conditions in absorbing water vapor and may be used to derive AET in hydrologic modeling (Dingman, 2002, p. 311-318).

PET itself can be calculated with temperature-based methods (Thornthwaite, 1948) or radiation-based methods (Priestley and Taylor, 1972). The simulation model employed in Chapter 3 relies on a water-balance model developed by Thornthwaite and Mather (1955) (see Steenhuis and Van der Molen, 1986), in which PET is calculated through a quasi-temperature-based approach resembling the Priestley and Taylor (1972) model (Dingman, 2002, p. 310). This approach utilizes the following semi-empirical equation:

$$PET = \frac{l}{\lambda} * \frac{s*(R_n - G)}{s+\gamma} * a \qquad (2)$$

Where α is the Priestley-Taylor coefficient, a constant value of 1.26, λ is the latent heat of vaporization (MJ kg^{-1}), R_n is net radiation (MJ m^{-2} day^{-1}), G is the soil heat flux (MJ m^{-2} day^{-1} (typically negligible in daily calculations), s is the slope of the saturation vapor pressure-temperature relationship (kPA $°C^{-1}$), and γ is the psychometric constant (kPA $°C^{-1}$). This formulation of PET offers the benefit of relying only on terms that are constants or can be calculated using air temperature and net radiation data, the latter of which itself can be estimated using minimum and maximum daily air temperatures.

AET, on the other hand, is the rate of ET that occurs at any site given potential water limitations and vegetation characteristics. Empirical measurements of ET recorded in the research that constitutes the following literature review are records of AET and, for this reason, this chapter will use the terms AET and ET interchangeably.

ET and soil moisture can be derived from PET by means of a Thornthwaite-type water-balance model (1955). Such models are used to simulate continuous watershed water input, soil moisture, and ET dynamics. To do this, the models lump water budget dynamics as discrete points, and capture spatially heterogeneous soil, topographic, and vegetation inputs as a single, representative parameter, typically regional soil-water storage capacity (SWC), calculated as:

$$SWC = \theta_{fc} * Z_{rz} \tag{3}$$

Where θ_{fc} is the field capacity, or the specific soil-water content below which the water drainage rate driven by gravity is reduced to some negligible level, and Z_{rz} is the depth of the root zone (Dingman, 2002, p. 235-238).

The total monthly or daily water input (W_m or W_d, respectively) to the budget is assumed to be the sum of P and snowmelt, the latter of which can be estimated through physically-based temperature snowmelt models (Walter et al., 2005). Finally, soil moisture (SW_t) for a given time period *t* is calculated:

$$SW_t = \min\{[(W - PET) + SW_{t-1}], SWC\} \; if \; W_t > PET_t \tag{4a}$$

$$SW_{t-1} - SW_t = SW_{t-1} * \left[1 - exp\left(-\frac{PET_t - W_t}{SWC}\right)\right] if \; W_t < PET_t \tag{4b}$$

Where, in Equation 4a, *SW* is assumed to increase in the case that W_t to the watershed exceeds local *PET*, unless the soil is already at *SWC,* and in Equation 4b, *SW* is assumed to decrease in the case that *PET* occurs at a greater rate than W_m.

JoFlow (Archibald et al., 2014), the model employed in Chapter 3 to simulate various aspects of hydrologic regime, calculates SW_t (similarly as described above) with the addition of two more terms:

$$SW_t = SW_{t-1} \exp\left(\frac{W_t - C_c * PET_t}{AWC}\right) if \; W_t > C_c * PET_t \tag{5a}$$

$$SW_t = SW_{t-1} + (W_t - C_c * PET_t) - D \; if \; W_t < C_c * PET_t \tag{5b}$$

Where C_c is a crop-specific coefficient to scale *PET* for various types of vegetation, *AWC* (mm) is the available water capacity across the watershed of interest, and *D* (mm) is groundwater drainage, which is calculated as in Equation 5c.

$$D = SW_{t-1} + (W_t - C_c * PET_t) - AWC \; if \; SW_{t-1} + (W_t - C_c * PET_t) > AWC \qquad (5c)$$

This model maintains W_d as a sum of daily P and snowmelt net daily Q, and as such requires Q data inputs, along with a catchment-specific value for AWC.

With the omission of groundwater and storage, changes in ET are captured with measured alterations of annual Q at any annual volume of P. The simplified equation can thus be expressed in the form:

$$P = ET + Q \qquad (6)$$

Of the terms in Equation 6, only annual P and Q totals can be measured accurately and, as direct measurement of ET is complicated, its value often is often derived indirectly (Hornberger et al., 2014, p. 40-52). ET measurements are possible at the canopy scale through either the calculation of the Bowen ratio or the use of the eddy covariance technique. However, these approaches are incapable of discerning between vapor fluxes from the ground surface and from vegetation, recording all-surface total ET contributions within a limited area (Eamus et al., 2006, p. 99). Conversely, field methods for calculating transpiration are limited to tree-level measurements that must often be scaled to the stand-level, as will be apparent in the review of the methodologies of research that constitutes the forthcoming literature review.

Further, both Bowen ratio and eddy covariance techniques are measurement and instrument intensive. Computation of the former, for example, requires the determination of temperature and water vapor concentration at two heights above the canopy, which can be

measured directly, as well as the estimation of eddy diffusivities of heat and water vapor, which is a more complicated process. The methodology may not always be appropriate for forest applications due to the relatively diminutive temperature gradient above tall canopies and the requisite fetch. Even where applicable, pairing calibrated and sufficiently sensitive temperature and water vapor sensors is a relatively involved task (Eamus et al., 2006, p. 100). Similarly, the latter approach demands the use of a hygrometer to record concentrations of water vapor at a point, a three-dimension sonic anemometer to gauge the velocity of the same current of wind (eddy) that passes through the hygrometer, and a sensor to log the temperature of the air sample. Although this is the sole approach for directly recording canopy gas flux, it delivers data characterizing bulk behavior of an approximately 1 km^2 area and is unable to discern between contributions by surface or vegetation type (Eamus et al., 2006, p. 101).

While some of the research reviewed later in this section employs the ET measurement techniques described to calculate fluxes at the stand or plot-scale, these direct approaches are unfeasible for the study presented in Chapter 3 given the sample size of catchments. Hence, changes in site-specific water budget are identified with Q, P, and temperature data available at a daily timestep through the United States Geological Survey (USGS) and National Oceanic and Atmospheric Administration (NOAA). Data describing site soil properties are gathered from the Natural Resources Conservation Service (NRCS).

It may be worth noting here that even the P and Q terms of the simplified water budget (Equation 6) are susceptible to some degree of measurement error. A common field method of measuring P is with a tipping bucket rain gauge, a device that consists of two buckets arranged in a seesaw (teeter-totter) arrangement such that they alternate fill-and-empty positions; the time of each “tip” is recorded and, knowing the bucket capacities, can be analyzed as a rainfall intensity.

Although gauge-based P data offer high temporal resolution, with records dating back far before the alternative satellite-based data acquisition systems were inaugurated in the 1970s, they are limited in their spatial coverage. Given the high spatial and temporal variability of P patterns, gauge-based measurements demonstrate a margin of error of ~10% (Winter, 1981; Wang and Dickinson, 2012), which may increase at higher data collection frequencies (Villarini et al., 2008).

Q measurements provided by the USGS are usually collected by siphoning water from a river into a stilling well, where the stage, or height, of water, which is equal to the stage of the running stream, is measured periodically with a float or a sensor (Sauer and Turnipseed, 2010). According to Wang and Dickinson (2012), the USGS estimates the margin of error of daily measurements acquired at a well-gauged stream to be ~5-10%. Not all stream cross-sections are well-gauged, however, and some datasets cover relatively short periods of time or are discontinuous in their record. To partially mitigate this issue, the simulation analysis presented in this study utilized only datasets that report a continuous record of discharge for at least 20 consecutive years.

The simplified water budget approach employed assumes direct relationships between P and ET, and P and Q, and an inverse relationship between ET and Q. This is in harmony with the principle of conservation of mass: an increase in rainfall volume must be followed by an increase in evapotranspiration or streamflow volumes, or both. However, these relationships are not direct or linear in nature. For instance, two vital indicators of hydrologic budget transformation in the present research are discharge patterns, but ecohydrologic determinants of Q generation are influenced by vegetation; soil characteristics; and geological topographical, and climatological factors (Wood et al., 2008b). To account for these spatially variable controls, Chapter 3

incorporates some site-specific vegetation, soil, landcover, and climate features as probable predictors of Q. It may be valuable at this point to briefly examine some of these features of plant-water relations at a more granular level, and review terminology that eventually appears in the research literature.

The volume of total water that is available for runoff and Q augmentation is partially determined by the water use regime of local vegetation. An important fundamental concept in tree physiology and soil physics is the Soil-Plant-Atmosphere Continuum (SPAC) model, which describes a hydraulic pathway from soil, to the roots, through the xylem and leaves to the atmosphere, across a thermodynamic gradient in water potential and additive internal physical resistances—or, inversely, conductance—within the plant. The water potential, Ψ (MPa), or the propensity of water to move from a place of low solute concentration to high solute concentration, is generally measured as the difference in free energy between a given solution and pure water (Philip, 1966; Kramer and Kozlowski, 1979, p. 405-406; Wood et al., 2008a).

There are a number of physiological controls that determine plant transpiration and, therefore, the balance of P available for surface runoff and infiltration, such as leaf area, root-to-shoot ratio, leaf orientation, and energy absorption. However, research suggests that at a coarser scale, the efficacy of the SPAC as a pathway is driven primarily by the environmental factors net radiation (R_n, Watts) and vapor pressure deficit (VPD, kPa). The latter term is a measure of the difference in vapor pressure or concentration between the leaf and the surrounding air. VPD sets the vapor pressure gradient along which water travels from the leaf interiors, a region of relatively higher vapor pressure to the air, a region of relatively lower vapor pressure. R_n promotes VPD by increasing leaf temperature and, consequently, leaf interior vapor pressure (Kramer and Kozlowski, 1979, p. 411; Bond et al., 2008; Brantley et al., 2013).

Another key internal plant process measured in some of the reviewed literature is stomatal conductance (g_s, mmol $m^{-2}s^{-1}$), or the rate of water vapor exiting leaf stomata. A plant's g_s is sensitive to light, measured as photosynthetic photon flux density or photosynthetically active radiation (PFD and PAR, respectively, mol $m^{-2}s^{-1}$ or μmol $m^{-2}s^{-1}$) to which it exhibits an asymptotic response. G_s is also responsive to VPD, with which transpiration generally has a positive linear relationship (that is, at low VPD levels, stomatal radius is maximized) up until a critical point after which transpiration arrives at some maximum ceiling (sometimes subsequently diminishing) and stomatal conductance declines exponentially (Bond et al., 2008).

It should be observed here that light-saturation points and critical VPD levels are species-specific. Empirical data indicate that conifers record lower values of light-saturation than broad-leaved trees and, further, that the sensitivity of g_s and transpiration to VPD depends on external drivers such as soil moisture and idiosyncratic hydraulic and anatomic characteristics that function to prevent cavitation or embolism (Ford and Vose, 2007; Bond et al., 2008).

Forest age and species composition also emerge as important regulating influences on stand-level ET rates and SW availability. Research evinces an inverse relationship between g_s (and therefore transpiration) and tree size, as longer xylem pathlengths render hydraulic transport more difficult. As such, old-growth forests have been found to exhibit both lower sapwood basal area and diminished stand-level transpiration rates relative to younger vegetation (Menzier et al., 2004; Moore et al., 2004; Bond et al., 2008).

Additionally, leaf area index (LAI, dimensionless), a ratio of a tree's one-sided leaf area to ground area, which increases with tree age, demonstrates a positive relationship with canopy interception, ergo an inverse relationship with rainfall incident at the forest floor and soil moisture during moderate and brief precipitation events (Bond et al., 2008). A higher canopy

LAI may to some extent limit transpiration by reducing soil moisture through interception. Beyond this, broadleaf species record higher daily transpiration rates relative to conifers during the leaf-on season (Menzier et al., 2004; Moore et al., 2004). These trends are particularly salient in the case of EH decline, as HWA infestation has been found to both shift mean foliage age to favor older growth and in the longer term, to precipitate a repopulation of extirpated EH stands by deciduous species. This sequence of transformations is likely of significant hydrologic consequence across different timescales (Ford and Vose, 2007; Brantley et al., 2013).

2.3 Immediate Hydrologic Consequences of Eastern Hemlock Mortality

Considering again the components of the water budget (Equation 6), and assuming a consistent P regime, EH mortality can potentially directly impact the local water budget through a reduction in ET and an increase in soil moisture, generating increased Q. This relationship is also nonlinear, as runoff can describe various pathways and processes that link available water, at different depths of the soil profile, to stream discharge. Hortonian overland flow (Horton, 1933), for example, augments stream volumes when the rate of P surpasses the infiltration capacity of the ground and, instead of infiltrating into the soil, excess rainfall flows over it. While this mechanism is relevant in urban and arid regions, where surfaces may be crusted, sealed, or impervious, it does not explain runoff formation in most forest soils of the Eastern coastal, Northeastern, and Southeastern regions of the U.S., which generally have higher infiltration capacities; in these regions, runoff is more frequently generated through saturation-excess overland flow via the generation of variable source areas (VSAs); the general premise being that saturated soils cannot hold additional water so excess P is routed as surface or shallow

subsurface flows (storm runoff). These saturated regions generally exist at low gradient, downslope positions in the landscape and can vary in their area, dilating or constricting based on antecedent moisture conditions and rainfall volume (Hibbert and Troendle, 1988; Ogden and Watts, 2000; Buchanan et al., 2018).

There may exist various additional controls and ancillary variables beyond runoff that impact the terms of the water balance equation and their mediating processes. However, this current conceptualization sets the broad contours for an investigation of HWA related ecohydrologic flux at a finer scale. The remainder of this section surveys existing research to synthesize a general understanding of the physical processes driving changes in ET, soil moisture, and runoff immediately following EH decline.

Gonda-King et al. (2014) investigated how HWA presence disturbs EH physiology by comparing growth of lateral and terminal branches, predawn shoot Ψ, photosynthetic processes, and g_s between experimentally infested and control tree samples (n = 15 per treatment) in Rhode Island. Trees in the control sample recorded 41% and 57% longer terminal and side branches, respectively; 45% higher predawn shoot Ψ (with a statistically significant negative correlation between HWA population and Ψ); and higher net photosynthetic rates and g_s (with a negative correlation between HWA population and g_s). These differences grew more pronounced over the course of the infestation. HWA presence, therefore, appears to potentially limit transpiration by impairing both plant structure and hydraulic function.

Domec et al. (2013) explored similar functional differences between HWA infested and healthy trees at a stand composed of EH and Carolina hemlock (*Tsuga caroliniana*) (CH) (n = 15 total, with n = 7 healthy and n = 8 infested) in North Carolina and scaled their findings to the stand-level. The researchers measured several tree attributes including predawn and mid-day leaf

Ψ, g_s, and branch-level, leaf-level, and stem xylem hydraulic conductivity. A partial account of all findings across the growing season (early June-late August) includes: Ψ gradients from soil to shoot were 43% and 49% lower in infested EH and CH trees relative to healthy trees, xylem hydraulic conductivity was reduced by 50% and 28% in infested EH and CH trees, respectively, and g_s was diminished in infested specimens by 40% in both species. All data were input to a soil-plant-atmosphere model, which simulates canopy-level fluxes with leaf-level parameterization. The model predicted a reduction in tree water use by 41% and 34%, wintertime (November-April) annual stand-level transpiration by 38% and 60%, and summertime (May-October) stand-level transpiration by 45% and 60%, for EH and CH, respectively. The authors further explained that xylem hydraulic impairment was the result of the growth of abnormal xylem cells caused by HWA outbreak, but that declines in sapwood conductance did not reduce whole-tree hydraulic conductance, due to an unexpected increase in leaf hydraulic conductance. Despite this, infested specimens suffered drought-like water stress and exhibited higher water use efficiency, and the investigators elucidate that this was likely due to a decrease in root to stem conductance.

Ford and Vose (2007) evaluated the impacts of EH mortality on stand-level transpiration rates at a riparian corridor where the foundation species constituted 50% of total basal area, located within the Coweeta basin in North Carolina. The researchers monitored 16 trees, measured sap flux density; generated whole-tree sap flow estimates through allometric scaling techniques; calculated local VPD, PAR, and PET from measurements of air temperature, relative humidity, wind speed and direction, and global radiation; recorded g_s to water vapor; and used some of the collected data to parameterize a model predicting changes in annual and seasonal stand-level transpiration at five stands without the presence of EH. Based on model results, the

investigators theorized that EH extirpation with no replacement from typical Southern Appalachian stands where the tree is a dominant species by basal area will lead to a reduction in annual-level transpiration by ~10% and winter and spring stand-level transpiration by ~30%. Further, Ford and Vose (2007) speculated that such a reduction in transpiration may result in increased SW due to diminished plant uptake and canopy interception, elevated Q, dilated VSA, and decreased diurnal amplitude of streamflow.

The results of these three studies suggest that HWA outbreak decreases tree water use and transpiration both through the direct impairment of the SPAC hydraulic pathway, as well as a shift to increase average foliage age (Stadler et al., 2005; Ford and Vose, 2007), which is inversely related to transpiration. These phenomena have the potential to increase SW availability and possibly, at least in the immediate aftermath of EH mortality prior to the establishment of any successional pioneer tree species, cause an increase in surface water runoff. While other research findings support the transpiration postulate, they remain divided about the effects of HWA on the total ET term, and on SW.

Lustenhouwer et al. (2012) examined the relationship between EH loss and various microclimatic factors at the Harvard Forest in Massachusetts, and their findings support the prediction of increased SW. The researchers monitored trends in light availability characterized as global site factor (GSF, a measure of the fraction of global radiation at a location relative to that in an open field), soil temperature, and summertime SW within two blocks. Each block consisted of four plots of which one was preserved as control dominated by hardwood species, one as a control dominated by EH, one dominated by EH was logged, and one dominated by EH was girdled. Some key study findings include: nearly equivalent GSF measurements in hardwood and EH control plots, but substantially higher GSF in treatment plots; a gradual but

significant increase in light availability during leaf-off periods only within the girdled plots; substantially higher initial SW values in treatment plots that decreased over time; and higher soil temperatures in the treatment plots with the greatest temperature difference between treatment and control plots occurring during the summer months.

Other studies conducted in Northeastern forests find no notable transformation in soil moisture levels. Jenkins et al. (1999), for example, compared various microclimatic and biogeochemical attributes between stands experiencing varying levels of HWA infestation (0% to 99%) located on uniform soil profiles (well-drained loamy) in Massachusetts and Connecticut. Measurements for their study included light availability characterized as canopy gap light index (GLI), soil temperature and moisture, and N cycling. The researchers reported significantly increased light levels at sites suffering infestation, but no differences in SW between infested and healthy EH stands.

Orwig et al. (2008) monitored eight sites where EH comprised >65% of the total basal area, suffering moderate to high levels of HWA establishment, but low overstory mortality, located on sandy loam, silt loam, and loam soils in Connecticut. The researchers measured microclimatic characteristics, GLI, net N mineralization, and N mobility. They interestingly reported that by the end of three years of study, infested stands exhibited lower SW levels at the forest floor and somewhat higher SW levels in the mineral soil, but that statistical analysis did not yield a significant relationship between HWA presence and the latter trend. Further, Orwig et al. reported no significant differences in either forest floor or mineral soil temperatures between infested and healthy sites. Despite this, GLI and overstory loss were found to exhibit a negative relationship with forest floor SW and a positive relationship with forest floor temperature. It

seems likely, therefore, that the sampling of stands experiencing low overstory mortality influenced soil temperature and SW level findings.

Royer et al. (2012) examined changes in near-ground solar radiation (< 1m above ground surface) engendered by drought-related overstory loss in the pinyon-juniper woodlands of northern Arizona. They measured annual and seasonal near-ground radiation fluxes, changes in solar radiation by initial canopy density classifications, and the relationship between solar radiation flux and altitude of canopy lost. The researchers reported an ~10% regional-scale average annual increase in seasonal radiation, a trend most conspicuous in the spring and summertime, and most pronounced increases in areas where canopies were initially denser and higher. This is a relevant finding as it suggests that overstory loss from EH stands, which are characterized by dense canopies (Brantley et al., 2013) at high altitudes, may result in higher near-ground solar radiation gains relative to some other species. While tree mortality response to invasive insect infestations may be more spatially heterogeneous than to drought, rendering the two phenomena imperfect analogues, several other studies concerned with HWA, specifically, support findings of increased light levels and soil temperature.

Eschtruth et al. (2006), for instance, in their longitudinal survey of EH plots in Pennsylvania and New Jersey over the course of HWA invasion found that total solar radiation, measured as understory light availability through hemispherical photography, doubled in nine years. Mladenoff (1987), in an analysis comparing N mineralization and its interaction with other measured soil characteristics between paired forest and tree gaps representing a species composition gradient from pure hardwood to EH dominated, recorded increased SW and temperature in gap plots.

In concert, this body of research supports that HWA outbreak impairs EH transpiration function, but a reduction of this component of the ET term of the water budget may not always be balanced by SW gains and therefore increases in Q. Instead, it is possible in some cases for heightened solar radiation input to the forest floor due to compromised canopy density to drive evaporative heat flux, which can offset decreases in transpiration, limiting SW levels and perhaps surface runoff contributions to Q.

Brantley et al. (2014) conducted a paired analysis between two catchments similar in topographic relief, soil characteristics, and disturbance history located in North Carolina. Both sites were experiencing HWA infestation, but differed in their species composition; EH comprised 6% of total basal area and 26% of riparian zone basal area of the study watershed, and <2% of the total basal area and 4% of the riparian zone basal area of the reference watershed. Observed Q data from the reference basin was regressed on expected Q at the infested basin under undisturbed conditions. Post-infestation, the regression model was used to predict water yield and storm responses, which were then compared with observed flow. The researchers found that over the study period, median annual water yield declined by ~9%, median monthly water yield declined by ~5% due mostly to hydrologic regime changes occurring during the dormant season, and median peakflow (or the point of maximum discharge following a precipitation event), decreased by ~12%, with a marginal decrease in growing season median peakflow and slight increase in dormant season median peakflow.

It should be noted, however, that the findings of this study were likely influenced by the considerably low prominence of EH in the study area, and previous research has demonstrated that changes in annual water yield typically follow >20% losses of basal area (Stednick, 1996; Brown et al., 2005). Further, Adams et al. (2012), in their review of ecohydrologic cascade

effects following tree die-off note that P regimes also control water yield responses: catchments experiencing ~500 mm P per year can be expected to deliver greater annual Q, while catchments receiving less than 500 mm will generally only do so if snowmelt is the preponderant contributor to P.

In other cases, researchers have described a marked increase in whole-catchment water yield corresponding with reductions in transpiration in the period immediately following HWA infestation (that is, prior to ecological succession) at the watershed scale. Kim et al. (2017), for instance, conducted a paired catchment analysis of two sites at Harvard Forest in Massachusetts experiencing HWA invasion but differing in their species composition. At one site, 41.1% of total area was comprised of >50% EH overstory, whereas at the other, only 18.7% of total area was similarly EH-dominated. The authors measured peak growing season (defined roughly as the summertime period June through August) daytime ET using flux tower measurements of eddies from wind-directions where 83% of total basal area consisted of EH. They studied the response of ET to PAR and VPD controls and recorded monthly Q data at the two sites. ET measurements were used to estimate canopy conductance as a function of HWA establishment, and the total data were used to parameterize and calibrate a mechanistic model that considers both plot-scale transformations with catchment-scale hydrologic processes to predict water yield both with and without the changes in the canopy conductance function. The researchers reported that over the period of study, ET decreased by 24-37%, corresponding with the 25-50% foliar loss resulting from HWA feeding, and simulated Q at the study site with a greater proportion of EH coverage increased by 15.6% as a result of the HWA-related canopy conductance function. Interestingly, the change in ET could not be accounted for by ambient variance in PAR and VPD, suggesting

that catchment-level water yield is a function of not only climatological factors, but also vegetation status.

One additional potential explanation for the relatively tenuous relationship between ET and VPD in this study could be that EH has not been found to exhibit a stomatal response to increasing VPD in order to maintain Ψ above some critical threshold to prevent adverse consequences such as cavitation. This is likely due to the fact that the species tends to grow in regions where it can access a stable supply of water either from generally higher SW or by drawing from the water table (Ford and Vose, 2007). Further, the tree's characteristically dense canopy cover and low transpiration rates, relative to hardwood species, reinforces cool, moist microclimatic conditions in the understory and at the forest floor (Catovsky et al., 2002). Hence, it may be possible that in the immediate aftermath of EH mortality, any marginal water gains of already moist soil are vaporized by net increases in solar energy input, especially in the upper soil horizons. This may indeed be the case for many of the studies that report no significant changes in SW. Over a longer term, following succession by other species, a restoration of transpiration can further mitigate any potential for surface runoff.

Studies comparing the isotopic signature of transpiration water from different tree species (Knighton et al., In Review) find that EH demonstrates greater root plasticity, drawing water from deeper soil horizons relative to American beech (*Fagus grandifolia*) (AB) when shallow soil water is limited. As much of the coastal Eastern and Northeastern U.S. exhibits VSA hydrology runoff generation and low catchment water storage (Walter et al., 2005; Buchanan et al., 2018), EH plant hydraulics may exert an important control on groundwater-fed VSA processes. EH mortality may therefore further reduce deep soil water uptake and catchment storage capacity, interacting with heightened precipitation in the late summer and fall seasons to

drive flooding risk (Knighton et al., In Review). This theorized trend, which would likely augment both Q volume and variability and may partially resolve the incongruencies between research that finds decreases in transpiration but no changes in shallow horizon SW, should persist in some measure even after the establishment of a successional species, if the pioneer differs in its rooting depth. To test this hypothesis, the modeling component of Chapter 3 explores baseflow trends, and erosion related parameters such as initial abstraction, a measure of the fraction of storm depth beyond which runoff commences, and hydrograph time-to-peak, a measure of the time between the onset of a precipitation event and discharge peak associated with the event.

Bearup et al. (2014) studied groundwater contributions to Q following mountain pine beetle infestation through chemical and isotopic hydrograph separation analysis, and their findings partially support the theory outlined just above. The investigators compared two watersheds in Rocky Mountain National Park, Colorado with uniform geologic, edaphic, and vegetation characteristics, but with differing levels of infestation. This study recorded increasing fractional contributions of groundwater to discharge over time at infested catchments, and higher groundwater contributions, on the order of 30 ± 15% at the site experiencing more advanced infestation, relative to the paired, neighboring basin. Through a water budget analysis, the authors further linked increases in groundwater runoff to decreases in transpiration related to invasive species outbreak.

2.4 Hydrologic Readjustments Following Ecological Succession

As EH populations decline across their native range, any transformations in established Q regimes will stabilize to new equilibria determined in some part by ET rates modulated by successional species. Transpiration contributes significantly to water cycling, estimated for example to be 30-40% water budget in the Southern Appalachians (Swift et al., 1975) and alterations of established regimes may be of significant consequence for the other terms of the hydrologic budget.

Generally, in stands where rosebay rhododendron (*Rhododendron maximum*) (RR) is present beforehand, EH decline provides an opportunity for this evergreen understory shrub, which impedes seedling recruitment, to dominate. In the absence of RR, field examinations have revealed that frequently the pioneer in Northeastern plots is the early successional black birch (*Betula lenta*) (BB), whereas in Southern plots it is red maple (*Acer rubrum*) (RM) (Orwig and Foster, 1998; Daley et al., 2007; Davis, 2008; Ford et al., 2011; Brantley et al., 2013). All three species differ from EH in water use, and light and P interception.

Davis (2008) studied transpiration rates, measured as sap flux density, of EH over a period of five years, and of RR, BB, and RM at plots located within the Coweeta basin in North Carolina where HWA presence was recorded. The researcher compared these data with PAR and D, and modeled different regeneration scenarios dominated by RR, BB, and RM. Local open-field solar radiation, air temperature, and relative humidity from a climate station was collected. Using these data, the investigator estimated PAR and VPD, determined sap flux density using thermal dissipation probes, sapwood area, and SW, calculated sap flow, compared

transpiration—quantified as changes in sap flux density over time—against PAR and VPD through a linear regression.

Finally, Davis (2008) simulated total stand sap flow in scenarios with baseline conditions, total sapwood area transition to RM, total transition to BB, and total transition to RR. Over the study period, sap flux density in EH exhibited a decline, although changes in later periods were insignificant. Regression coefficients indicated that sap flux density for EH would decline over time, remain stable for RM, BB, and RR at any values of these climatological factors. Finally, simulation determined that in the case of succession by RR, the shrub's specific transpiration rates will likely increase, but still remain lower than typical sap flow rates for EH; in the case of total sapwood area replacement by RM, total sap flow may increase by ~38.3%; in the case of total sapwood area replacement by BB, total sap flow may increase by ~71.2%; in the event that successional composition is evenly distributed between RM and BB, total sap flow may increase by ~54.8%. On the basis of these results, Davis predicted an overall increase in total annual sap flow following EH replacement by the deciduous species examined, but a significant reduction in winter and early spring sap flow.

Brantley et al. (2013) conducted a study in the same basin, estimating ET during an ongoing HWA infestation and under future conditions following succession at stands where EH constituted 50-60% of total basal area. The authors collected local open-field air temperature, relative humidity, rainfall, and solar radiation data from the same climate station as Davis (2008). They estimated PFD and VPD from this data, measured climate variables at each of the study plots, determined SW, and gathered sap flux density data for EH (n = 16), BB (n = 7), RM (n = 3), RR (n = 6), using constant heat thermal dissipation probes for a period of a year (although not all concurrently). Further, they determined sapwood area and leaf area using

allometric relationships, as well as leaf-level transpiration (EL) rates through the combination of leaf area and sap flux data.

Brantley et al. (2013) also studied the relationship between each of the climatic variables (air temperature, VPD, PFD, and soil moisture) and leaf-level transpiration, and found that: BB demonstrates substantially higher EL than the other species studied at all times but the winter months; RM EL is higher than EH EL during spring and summer months; mean EL for EH and RR do not disagree significantly; and D and PFD are the first- and second-best predictors of EL for all species, respectively. At stand-scale, EH was found to be the largest contributor to annual ET (at 25.9% of total) prior to HWA outbreak, despite its relatively low EL, supplying 74% and 52% of winter and autumn ET; while interesting, and ostensibly conflicting with Davis (2008), this result may be due to the large population of EH trees within the stands from which data were sampled. Indeed, BB, although comprising a significantly lower fraction of total leaf area than EH, contributed 23.1% of total annual ET. Simulation results indicated that with ecological succession, annual stand-level ET should return to pre-infestation (2004) levels by 2020 and surpass this value by 12% by 2050. However, due to the seasonal restructuring of the ET regime, with the cessation of transpiration by deciduous pioneers during the leaf-off period and the relatively lower contributions by RR, winter ET may only recover to 38% of 2004 values by 2050, accounting for 2.8% of total annual ET. Brantley et al. predicted a decline in Q, a trend likely to be most concentrated in the leaf-on period, and possibly an increase in winter Q, as a result of decreased ET during the leaf-off months. The authors further posited that as BB in the Southern Appalachians enjoys a longer growing season and higher temperatures than in Northeastern states, hydrologic modulations resulting from a replacement of EH by BB may be more pronounced in the South, causing shifts in SW and Q levels.

In an investigation conducted at Harvard Forest in Massachusetts, Daley et al. (2007) reported ET rate differential trends between EH and BB consistent with those from the studies located in the Southern Appalachians. The researchers designated two sites, one in which EH comprised 84% of total basal area and one of mixed deciduous composition dominated by red oak (*Pinus strobus*) (RO), but in which BB can be found, and collected sap flux measurements from individual trees (n = 8 for each species) through constant heat sap flux sensors. Rather than scaling data to obtain whole-tree measurements, the investigators eschewed the assumption of constant sap flux through the entire conducting area, noting that such a methodology may neglect that in some species, sap flux velocities increase radially outward from inner sapwood. They accordingly utilized inner sap flux sensors in some specimens constituting their sample (n = 3 for each species) and subsequently calculated sap flows. Using the eddy covariance approach, the investigators collected stand-level ET measurements at each site and determined the relationships between ET and VPD, and ET and PAR.

Research results included the following: PAR and VPD determined 60-70% and 20% of ET fluxes at each study site, respectively; nocturnal minimum temperatures modulated EH stand water use; mean ET at the deciduous forest during the leaf-on period was nearly double that at the EH forest; the deciduous stand maintained water use patterns comparable to the EH stand in the winter and spring, despite leaf abscission in the former; annual forest water use was 90-100 mm higher at the deciduous forest in all years of the study; and seasonal mean, total daily, and peak transpiration rates were substantially higher in BB specimens during the leaf-on period, a trend that reversed during the winter months, following an inflection point in August. The authors postulated that the similarity in ET rates between the two sites during the winter months was likely due to a suppression of ET from the shaded understory of the EH forest, and a

sustenance of ET, despite lack of overstory canopy, from the irradiated understory of the deciduous forest. They further predicted that in the event of a stand-level transition from EH dominance to BB dominance, ET gains may present a threat to the sustainability of growing season Q in neighboring streams; despite the year-round transpiration activity exhibited by EH, results from this research suggest that at Harvard Forest, annual ET activity from EH dominated stands does not surpass that from mixed deciduous stands.

This study is significant in that rather than approximating forest ET from tree-level measurements, Daley et al. (2007) pursued higher scale data through the eddy covariance technique. This allowed the researchers to distinguish between tree water use differentials and forest-scale vapor fluxes, and to identify overall changes in ET due not only to transpiration specific to the species of interest, but also to co-occurring species and other environmental factors such as seasonal light availability patters.

In concert, the results of the three studies outlined in this section advance the thesis that EH sap flow activity may be periodically occluded in Northern latitudes where seasonal and daily minimum temperatures tend to be lower than in Southern regions. While this suggests that hydrologic consequences of increased ET following EH decline and forest regeneration may be muted in Northeastern stands relative to Southern counterparts if P regime is unaltered, the Northeast U.S. is experiencing an increase in extreme precipitation (Frei et al., 2015; Huang et al., 2017), hydrologic response to which may be supplemented by EH loss.

Daley et al. (2007) acknowledge that the deciduous forest ET data were collected at a stand where RO, and not BB, was the dominant species. However, review of other research indicates that RO transpiration rate corroborates the general predictions of stand transition repercussions offered by Daley et al. For example, Catovsky et al. (2002) estimated canopy

conductance using sap flow rates obtained from RO, RM, and EH located at Harvard Forest, and reported that, despite the seasonal controls on the sap flow activity of the deciduous species, these trees demonstrated two to four times higher annual transpiration per ground area than EH, with RO further surpassing RM by 60-80%. The researchers further postulated that EH removal from mixed temperate stands may drive a two to four-fold whole-forest water loss.

Finally, Daley et al. (2007) invoked the water balance concept and argued that any transpiration gains must be balanced by inverse effects Q, groundwater contributions, or storage, but acknowledged that their methodology did not account for variations in interception between EH and BB, a mechanism that is indeed of import to hydrologic regime transmutation. While higher canopy densities may suggest greater interception efficacy by EH trees relative to deciduous species (Guswa and Spence, 2012), this supposition omits more complicated, nonlinear phenomena, such as throughfall, which can exercise a delayed impact on water budget through SW (Schume et al., 2003).

Guswa and Spence (2012) identified that persistent spatial patterns of SW resulting from P partitioning can be linked to species-specific vegetation structure, eventually exerting partial control over recharge and transpiration. Therefore, transition from EH to other tree species may modify water budgets vis-à-vis throughfall modulation. The authors applied a stochastic model treating P events as Poisson events and mathematically expressing the P-to-SW process in two stages. Initially, individual P observations were partitioned into either interception evaporation or throughfall phenomena based on event depth. For the subset of P observations that qualified as throughfall events, distributions for each spatially explicit location were then determined through a local mean event depth generated from a Gamma distribution and a separate coefficient of variation. Subsequently, these two location-specific parameters, mean event depth and the

coefficient of variation, along with potential transpiration, root depth, and AWC, were used as inputs to an equation to calculate transpiration. These data were then spatially integrated to produce estimates of stand-level mean transpiration and SW recharge. Beyond the modeling component of their research, the investigators gathered empirical measurements of throughfall at an EH and a deciduous stand with the aid of simple receptacles.

Guswa and Spence (2012) reported that: spatial variability of throughfall is positively related to net recharge, as potential transpiration rates serve as an upper bound for plant uptake; regions where SW is already high will contribute any additional water input to recharge, indicating that the recharge process is a function of both the volume of interception and the spatial redistribution of incident water by the canopy; P partitioning and spatial redistribution may persistently concentrate SW recharge in specific regions; throughfall signatures produced by the two stands studied differed in both volume and spatial pattern, with the deciduous forest exhibiting lower mean interception relative to EH and producing distinct regions of high SW, and EH conversely producing regions of low soil water content; and, finally, higher transpiration rates characteristic of the deciduous stand voided any effects of interception, as even though a greater fraction of P arrived at the forest floor in the deciduous forest, it was lost to plant uptake.

Although the phenomenon was not observed in this study, applying the VSA concept, in the event that transpiration processes do not overwhelm the creation of regions of concentrated SW, water input may indeed increase surface runoff and Q, but no studies were found that verify this process empirically. Guswa and Spence anticipated reduced SW recharge and Q during the summer months following the replacement of EH with deciduous vegetation, which is congruent with the other studies reviewed (e.g., Brantley et al., 2013; Knighton et al., In Review).

However, Roberts et al. (2009), in surveying differences in several variables for a study that paired streams draining EH dominated and hardwood dominated basins located in the Great Smoky Mountains National Park, found species composition to be a poor indicator of stream characteristics. The investigators utilized a 10-meter spatial resolution digital elevation model to determine stream-pairs within catchments with minimal difference in disturbance histories; geologic classifications; atmospheric deposition; and topographic features emergent across stream channel, riparian buffer, and whole-catchment scales. For each site, the researchers gathered data describing PAR, stream water temperature, nitrate levels, pH, and discharge, and found no significant differences in any of the variables except for PAR, but that was only during the leaf-off period, which is to be expected. Based on these results, they argued that at a catchment-scale, a transition from EH to deciduous pioneers may be of no significant hydrologic or hydrogeochemical consequence, but smaller-scale effects may be more pronounced.

2.5 Synthesis of Reviewed Literature

It is apparent that the ecohydrologic outcomes of HWA infestation are difficult to generalize and predict, muddled by confounding factors inconsistent in both space and time. Indeed, hydrologic fluxes incepted at the onset of infestation may exhibit general trends specific to their geographical location, but these trends continue to permute over the course of EH decline, mortality, and replacement.

Given the heterogeneity of forcing factors that may determine the final hydrologic outcome of EH mortality, arriving at a general theory relating HWA outbreak with water balance fluctuation and rebalance is an improbable aspiration. Yet, synthesizing the body of past research

results yields a few key points that can supplement the interpretation of results yielded by statistical and simulation modeling in Chapter 3:

1. In the short-term, prior to ecological succession, a reduction in canopy storage as a result of EH extirpation by HWA may drive an increase in both shallow and deep soil moisture levels. In the upper soil horizons, this effect may be balanced by heightened evaporation as a result of increased solar radiation at the forest floor.
2. Irrespective of forest floor light availability, EH mortality may increase deep soil water contributions to stream discharge, driving variable source area runoff effects and streamflow regime volatility.
3. Catchments that are located within the native EH and HWA outbreak range are likely to report increases in streamflow volumes and flow regime volatility, and decreases in ET as a proportion of bulk P, relative to catchments within native EH range but outside of HWA range.
4. Considering all overland and subsurface runoff processes together, catchments experiencing HWA infestation are likely to exhibit mechanistic trends indicative of increased flooding potential, such as a reduction in hydrograph time-to-peak, initial abstraction, and catchment water storage capacity.

CHAPTER 3

SIMULATION AND STATISTICAL MODELING APPROACHES TO INVESTIGATE DOMINANT CONTROLS ON HYDROLOGIC REGIME TRANSFORMATIONS FOLLOWING EASTERN HEMLOCK MORTALITY[1]

3.1 Introduction

Ecological and hydrologic processes in forested ecosystems are often dependent on the functional and structural roles of foundation tree species (Brantley et al., 2017)—regionally abundant specimen varieties generally occupying lower trophic levels that maintain stable conditions within their embedding environments (Ellison et al., 2005). Ecohydrologic controls on the critical zone are strongly influenced by Eastern hemlock (*Tsuga canadensis*) (EH), one such foundation tree species present throughout much of the Northeastern and Southeastern U.S. EH regulates the hydrologic cycle by sustaining root water uptake and transpiration through all seasons and maintaining consistent spatial patterns of throughfall, thereby possibly modulating soil moisture, groundwater recharge, baseflow regime, and stream discharge (Snyder et al., 2002; Stadler et al., 2005; Daley et al., 2007; Ford and Vose, 2007; Guswa and Spence, 2012; Brantley et al., 2013; Brantley et al., 2014; Kim et al., 2017; Knighton et al., In Review).

Forest communities dependent on EH-regulated microclimatic conditions are threatened by the hemlock woolly adelgid (*Adelges tsugae*) (HWA), an invasive insect that feeds on starch

1 Singh K., Knighton J., Whitmore M., Walter M.T., Lassoie J.P. In Review. Simulation and Statistical Modeling Approaches to Investigate Dominant Controls on Hydrologic Regime Transformations Following Eastern Hemlock Mortality. Hydrological Processes.

reserves found in the parenchyma cells of EH twig xylem (Young et al., 1995). HWA infestations progress rapidly both spatially and temporally. The insect was first reported in the Southern Appalachians in the 1950s (Ford et al., 2011) and its range has since extended across the Eastern coast of the U.S. (Brantley et al., 2014). HWA feeding results in the mortality of developing EH buds, precluding the production of new foliage. Although the rate of EH decline following the onset of infestation varies depending on a variety of context-specific factors such as EH stand size and density, soil type, and mean annual temperature, past studies have recorded mortality in as little as four years (e.g., Young et al., 1995).

Examinations of EH tree physiology within the range of an HWA outbreak have found a reduction in tree stomatal conductance and decreased root to stem conductance, likely a result of root embolism following a diminishment of water potential (Domec et al., 2013; Gonda-King et al., 2014). As previous studies have suggested that EH serves an important function with regards to the water cycle, in part as the preponderant contributor to transpiration during leaf-off months, loss of this species, or a vitiation of its hydraulic properties, is projected to cause significant seasonal shifts or declines in catchment actual evapotranspiration (ET) (Stadler et al., 2005; Daley et al., 2007; Ford and Vose, 2007; Adams et al., 2012; Brantley et al., 2013; Kim et al., 2017; Knighton et al., In Review).

Research finds that HWA infestation induces a reduction in water use in infested stands by >40% (Domec et al., 2013) and EH mortality diminishes annual stand-level transpiration by ~10%, and winter and spring stand-level transpiration by ~30% in typical Southern Appalachian forests, where HWA populations are more established relative to the Northeast (Ford and Vose, 2007). In forests where EH comprises 50-60% of total basal area, Brantley et al. (2013) report reductions in annual and winter ET by 22% and 74%, respectively. Studies have also noted

increases in throughfall volume and a distortion of throughfall spatial distribution pattern—phenomena inversely related to net recharge—as a result of decreased canopy interception (Stadler et al., 2005; Guswa and Spence, 2012).

These primary effects of EH die-off could possibly engender various indirect consequences for soil moisture and streamflow timing and volume across different temporal and spatial scales. Given unaltered precipitation patterns and a reduction in ET, more water may be available for infiltration and groundwater recharge, overland flows, and shallow subsurface flows, with partitioning between these processes occurring in accordance with such interacting contextual factors as soil profile and infiltration capacity, and water table depth (Adams et al., 2012). There is some evidence that EH loss will precipitate increases in rooting zone soil moisture and annual catchment water yield, along with associated decreases in daily amplitude of stream-flow and a dilation of variable source areas (VSA) (Ford and Vose, 2007; Lustenhouwer et al., 2012; Kim et al., 2017; Knighton et al., In Review). Prior studies also provide some evidence of an overall increase in annual ET rates over a longer time period, particularly in the summer months, as ecological succession replaces extirpated EH stands with tree species exhibiting higher transpiration rates (Daley et al., 2007; Hadley et al., 2008).

It is important to note that studies investigating the ecohydrologic repercussions of tree die-offs, in general, are few (e.g., Adams et al., 2012), and research surveying the hydrologic consequences of EH mortality specifically is limited to tree or plot-level investigations (Daley et al., 2007; Ford and Vose, 2007; Hadley et al., 2008; Lustenhouwer et al., 2012; Domec et al., 2013), with few appraising catchment or watershed level fluxes (Brantley et al., 2014; Kim et al., 2017). Given the complex relationships between canopy interception, unsaturated and saturated groundwater storage, and root water uptake, it is not immediately clear how EH loss will carry

over into the hydrologic cycle. A decline in EH stand density could impart non-linear changes to stream discharge as observed by Brantley et al. (2014), although whether the spatial range of this effect extends beyond Southern Appalachian forests is uncertain. Due to the context and scale-dependent nature of existing research, it is difficult to extract from its findings a generalizable understanding of how HWA infestation impacts catchment hydrology. For example, it is possible that observed hydrologic impacts of the HWA may be more pronounced in typical Northeastern forests, particularly those in New England and upstate New York, than in Appalachian forests, as the former often feature higher densities of EH (Albani et al., 2010).

It is necessary, however, for forest and watershed management efforts to have an approximate understanding of the broad hydrologic phenomena that are likely to result from HWA infestation, which may not be obvious from the research literature. The objective of the research presented in this chapter is to evaluate, at a regional scale, relationships between fluxes in catchment water balances and the condition and presence of EH stands throughout the Southeastern, Northeastern, and Midwestern U.S. utilizing long-term hydrologic records. This study addresses the following questions:

1. Does EH infestation impart changes to ecologically relevant stream discharge characteristics across the Eastern U.S.?
2. Does EH infestation functionally change how catchments partition precipitation into baseflow and surface runoff across the Eastern U.S.?

Previous studies examining the role of forest cover as a control on flooding frequency predicated on statistical methodologies have produced inconsistent outcomes of varying

statistical significance (Bradshaw et al., 2007; Li et al., 2016; Tan-Soo et al., 2016; Brogna et al., 2017). For example, an econometrics-based examination of flooding risk in Malaysia (Tan-Soo et al., 2016) found weak relationships between the monthly flooding frequency response variable and all land-use classification explanatory variables considered; the only exception was urban cover, which may be more indicative of flood reporting correlated with higher population densities in urban areas than physically-based ecohydrological relationships. On the other hand, in another multi-catchment statistical analysis based in Belgium, Brogna et al. (2017) discovered relatively less tenuous correlations between hydrologic response variables and forest cover.

On a global scale, Bradshaw et al. (2007) demonstrated a positive relationship between flooding frequency and natural forest area decline, but in a reanalysis of their data, Van Dijk et al. (2009) emphasized its various limitations and identified confounding explanatory factors that suppress the hydrologic role of forest cover substantially. Beyond this, Bradshaw et al. relied on oversimplifications of dynamic physical phenomena, such as their assumption of randomly generated country-scale antecedent soil moisture values, which are in fact heterogenous over much smaller geographic scales and vary temporally with external factors such as preceding rainfall.

Given the inconsistencies in conclusions regarding the significance of the role of forest cover in flood mitigation across these previous studies, the present research also seeks to understand if methodological limitations are possibly mischaracterizing the influence of forest composition on catchment hydrology. Therefore, the questions presented above are addressed within the context of three models, which vary in their assumptions, and in the extent of knowledge of catchment hydrology carried forward to help explain variance in the observations. First, a parametric statistical analysis (i.e., a multivariate linear regression) is performed utilizing

a suite of common catchment characteristics and EH infestation condition (healthy or infested) to determine if HWA outbreak can be identified as a significant influence on the discharge regime. Then, a non-parametric statistical test (i.e., Kolmogorov-Smirnov) is employed to evaluate differences in hydrologic regime trends between healthy and infested catchments. Finally, a physically based hydrologic simulation model is used to determine the influence of EH condition on optimal model calibration parameter values.

3.2 Methodology

3.2.1 Description of Regional Hydroclimate and Datasets

Eighty-one daily streamflow records were collected from the U.S. Geological Survey (USGS, 2018) across 17 U.S. states based on the availability of at least one full year of flow data; 42 sites recorded measurements from January 1, 1980 to December 31, 2016. Hence, the most temporally expansive datasets span 37 years of daily measurements, whereas the shortest, a subset of four sites, span between 2-3 years. The mean and median record length for all gaging locations are 27 years and 37 years, respectively. Streamflow data were collected via the EcoHydRology package for the R scripting language (Fuka et al., 2018). Selected gauging stations are presented in Figure 1.

Sites were organized between two broad categories: within native EH range with no reported HWA presence (healthy, n = 37), and within native EH range with reported HWA presence (infested, n = 44), based on the spatial classification of HWA range (USDA Forest Service, 2018). Importantly, this binary classification does not capture the extent or duration of

infestation, only that HWA presence has been observed. Further, the presence of additional tree species within the study region likely introduces confounding variance.

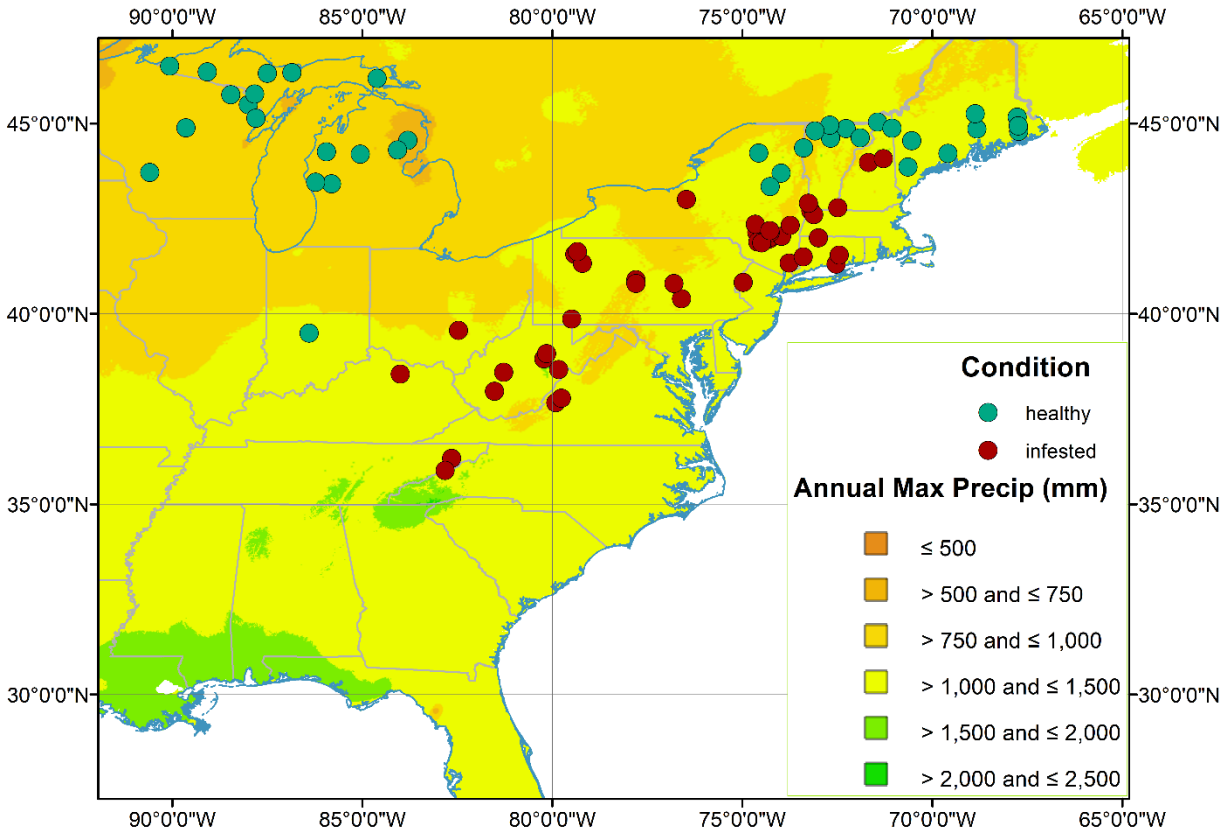

***Figure 1**: Distribution of healthy and infested sites by geographic location.*

Soil textures and physical properties, specifically available water capacity (AWC) and saturated hydraulic conductivity (K_{SAT}), were gathered for the most dominant soil type at each stream discharge gaging station location from the Natural Resource Conservation Service Soil Survey Geographic Database (SSURGO) (Soil Survey Staff, 2017).

Daily precipitation and mean annual precipitation (MAP) for each site were gathered for the period 1976-2017 from the Climate Prediction Center (CPC) Unified Gauge-Based Analysis of Daily Precipitation over CONUS, a 0.25-degree precipitation product derived from a dense network of precipitation gaging stations (Chen et al., 2008). Daily minimum and maximum temperatures and Mean Annual Temperature (MAT) for the period 1979-2017 were sourced from the CPC Global Daily Temperature dataset, a 0.50-degree product. All CPC data are provided by NOAA/OAR/ESLR PSD Boulder, Colorado, U.S. (2018).

Land-cover composition was referenced with the 2011 National Land Cover Database, a land-cover classification product at 30-meter spatial resolution that organizes cover into 16 distinct categories (Homer et al., 2015). Watershed boundaries were determined for each site using a HUC12 map from the national Watershed Boundary Database (USGS, 2018). The landcover map was clipped to the hydrologic unit boundaries of each gauge site. The percentage of total area each landcover type contributes for each catchment was calculated, and the percentages of evergreen, deciduous, and mixed forest cover were recorded (Anderson et al., 1976). Histograms of site characteristics are presented in Figure 2, demonstrating similarity between infested and non-infested grouping of catchments. MATs and MAPs across the infested subset of sites are higher than healthy; the average MAT and MAP across infested sites are ~9.06°C and ~1,185.8 mm, and across healthy sites are ~6.13°C and ~1,003.15 mm, respectively. This is likely due to the location of healthy sites at higher latitudes (mean of ~44.68°N and median of ~44.81°N) relative to infested sites (mean of ~40.94°N and median of ~41.56°N). The distribution of infested sites favors slightly higher catchment area, and lower K_{SAT} and AWC, recording means of ~1,912 km^2, 2.08 cm/hr, and ~137.8 mm, respectively, relative to the means for healthy sites of ~1,578 km^2, 3.5 cm/hr, and ~159.6 mm, respectively.

Healthy sites, while characterized by lower forest cover (mean of ~60.8%) relative to infested sites (mean of ~71.8%), record on average twice the evergreen forest cover as a percentage of total land cover, at ~12%, relative to infested sites at ~5.9%. This may be a manifestation of HWA outbreak in some measure, considering that ecological succession dynamics were limited by organizing sites that may now feature deciduous vegetation replacements of previous EH stands within the infested category, but this coarse analysis cannot ascertain physical characteristics at each sampled site.

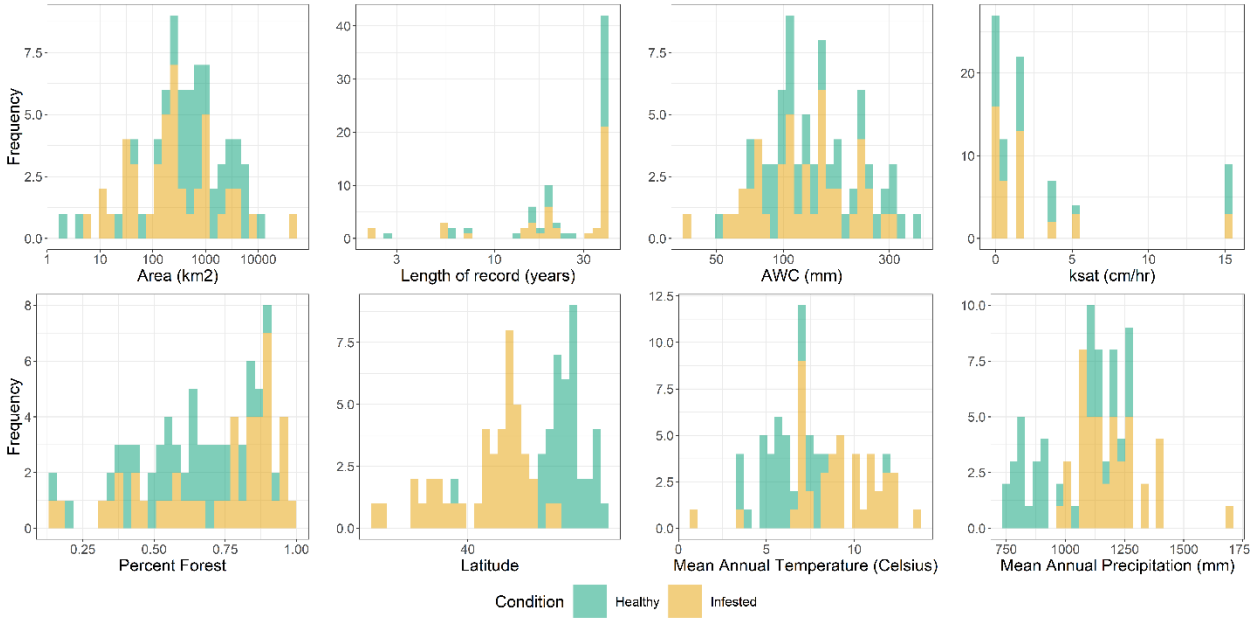

Figure 2*: Stacked histograms of catchment characteristics across the total set of 81 USGS gauge sites.*

Further analysis of the catchment characteristics data with the two-sample Kolmogorov Smirnov test (explained further in section 3.2.3.2) revealed statistically significant differences (p-

value < 0.05) in the distribution of catchment area, forest cover, latitude, MAT and MAP, with infested sites featuring a lower area, and higher forest cover, MAP, and MAP.

3.2.2 Flow Data Characterization

Daily streamflow data at all sites were characterized as three ecologically relevant indices: Richards-Baker Flashiness index (R-B) (Baker et al., 2004), baseflow index (BFI), and the ratio of total ET to total precipitation (ETP). R-B, a measure of the frequency of short-term changes in stream-flow patterns, was calculated following the methodology of Baker et al. (2004), which measures the ratio of discharge oscillations to total discharge as:

$$\frac{\sum_{i=1}^{n}|q_i - q_{i-1}|}{\sum_{i=1}^{n} q_i} \quad (7)$$

Where q is mean daily flow, and i is a single time-step. The R-B is an indicator of hydrologic regime volatility and can be used to assess ecohydrological changes to discharge. Numerically, R-B exists within the range (0, 2), where higher values suggest greater flashiness or streamflow volatility.

Changes to stream baseflow, the component of total discharge that is generally attributed to groundwater baseflows as opposed to storm runoff contributions and is thus less sensitive to precipitation patterns, were quantified as the BFI (e.g., Eckhardt, 2008), or the ratio of total baseflow to total discharge. The baseflow separation function of Nathan and McMahon (1990), as implemented in the EcoHydRology package (Fuka et al., 2018), was used to separate baseflow

volumes from the discharge record. Higher values of BFI indicate a lower contribution of storm runoff to total discharge and that the stream likely exhibits less regime volatility.

ETP for all sites was estimated as the difference between annual precipitation and annual streamflow divided by annual precipitation during the period 1976-2017 from CPC data (2018), under the assumption that changes to intra-catchment water storage are small compared to annual fluxes in P, Q, and ET. For this calculation, precipitation data for all sites missing a concurrent discharge measurement were omitted.

3.2.3 Statistical Approaches to Estimating Forest Cover Influence on Discharge

3.2.3.1 Multivariate Regression of Ecologically Relevant Streamflow Characteristics

All statistical and simulation analyses and data visualization were performed using RStudio version 1.1.456. First, the influence of EH infestation on the previously described ecological streamflow indicators was assessed via multivariate regression analysis. Three general multivariate regressions of the form below were parameterized:

$$y_i = \beta_1 x_{i1} + \cdots + \beta_p x_{ip} + \varepsilon_i \tag{8}$$

Where the response variable y_i took the value of either the calculated R-B, BFI, or ETP, and the regressors took the values of physically meaningful catchment characteristics (Table 1). Through this, relationships between the classification of healthy and infested EH forests and the ecologically relevant flow characteristics R-B, BFI, and ETP were identified.

Regressor	Description	Source
condition	Classification of site as '1' if located both within EH and HWA range, and '2' if located within EH range but outside HWA range	Little, 1971; USDA Forest Service, 2018
area	Area of watershed within which gauge is located	USGS, 2018
lat	Geographic latitude of gauge location	USGS, 2018
K_{SAT}	Saturated hydraulic conductivity, or the rate at which the saturated soil transmits water	Soil Survey Staff, 2018
AWC	Available water capacity, or the capacity of soil to hold water	Soil Survey Staff, 2018
MAT	Mean annual air temperature at site	CPC Global Daily Temperature (2018)
MAP	Average precipitation at site	CPC Unified Gauge- Based Analysis of Daily Precipitation over CONUS dataset (2018); Chen et al. (2008)
Percent forest	A summation of landcover classified as deciduous, evergreen, and mixed forest	Anderson et al., 1976; Homer et al., 2015

Table 1*: Hydroclimate and physical catchment characteristics used as covariates within the multivariate regression analysis.*

3.2.3.2 Kolmogorov-Smirnov Two-Sample Test

Next, empirical cumulative distribution functions (CDFs) generated with R-B, BFI, and ETP indices data across both healthy and infested sites were analyzed with the two-sample Kolmogorov-Smirnov (K-S) test. The K-S test is a non-parametric measure of distribution equality that determines the difference between two probability distributions through a measure of the maximum vertical distance between CDFs generated from the distributions. As the distribution of the model parameter sets cannot be predicted *a priori*, the K-S test is suitable as it imposes no assumptions related to the underlying theoretical distribution of the test data. The

null hypothesis of this approach is that both CDFs are drawn from the same data generating process (i.e., no influence of HWA infestation on flow partitioning). The alternate hypothesis proposes that all observations are produced from distinct data generating processes. Rejection of the null hypothesis would provide evidence for EH infestation imparting some effect on flow partitioning and the processes that generate surface runoff. A test statistic (Ds) that represents the distance between two CDFs was calculated, and significance was predicated on three subjectively selected p-value thresholds of 0.05, 0.10, and 0.20 (Hornberger and Spear, 1981).

3.2.4 Hydrological Model Development

To further investigate the extent to which HWA infestation affects storm runoff and stream discharge patterns, a 45-site subset of the full sample of 81 watersheds, consisting of 20 healthy catchments and 25 infested catchments, was generated. Flow partitioning at each of the gauge-sites within this subset, which exhibited continuous daily streamflow records for the 20-year period from January 1, 1997 to December 31, 2017, was analyzed using the Lumped VSA model, JoFlow (Archibald et al., 2014). JoFlow is a semi-physically based hydrologic model that maintains a lumped daily water budget at the catchment scale while spatially distributing runoff processes. Potential Evapotranspiration (PET) and snowpack accumulation and melt dynamics were physically simulated following Archibald et al. (2014) and Walter et al. (2004), respectively. Within JoFlow, surface runoff is solved via a modified Curve Number-like approach and vadose zone dynamics and ET are determined through the daily Thornthwaite-Mather soil water budget (Thorthwaite and Mather, 1955). JoFlow was selected for its low

dimensionality and the inclusion of relevant hydrological processes (Knighton et al., 2017a, b; Georgakakos et al., 2018).

Forcing data supplied to the model consist of latitude (USGS, 2018), daily precipitation, and daily minimum and maximum air temperatures. Unsaturated zone AWC and depth to confining layer were determined from SSURGO (Soil Survey Staff, 2018). A consistent albedo value of 0.23 was assumed for non-snow cover conditions across all catchments. During snowpack accumulation and melt, surface albedo was modeled following Walter et al. (2004).

JoFlow hydrologic model parameters for each catchment (both infested and healthy) were calibrated using the Dynamically Dimensioned Search (DDS) algorithm (Tolson and Shoemaker, 2007). Model calibration parameter descriptions and feasible ranges are presented in Table 2.

The calibration parameter set for each catchment that maximized the predictive power of the model was preserved. Predictive power was determined by the daily discharge Nash-Sutcliffe Efficiency (NSE) coefficient (Nash and Sutcliffe, 1970), following 10,000 iterations of parameter value selection through Monte Carlo sampling of parameter values from uniform distributions within indicated boundaries.

Parameter	Boundary Range	Description
forest	(0,1)	fraction of forest cover within catchment
Tp (hours)	(0,4)	Time to peak (hours)
Ia (mm)	(0.05, 0.9)	Initial abstraction (mm)
PETmax (mm)	(2,10)	Maximum daily PET (mm)
percent impervious	(0,100)	fraction of impervious cover
rec_coef	(0.0001,0.2)	baseflow recession coefficient
C1	(1,5)	parameter relating storage to soil water deficit
Se_{min}	(40,210)	minimum daily catchment storage

***Table 2**: JoFlow model parameter values and ranges.*

CDFs of all calibrated model parameters as estimated for healthy catchments against those estimated for infested catchments were compared, relying again on the two-sample K-S test. This approach potentially provides further insight into the mechanisms of runoff generation.

Note that selection of the sampling ranges of hydrologic parameters is a critical issue in sensitivity analysis, and hydrologic model parameter ranges for this research were selected following other studies utilizing JoFlow (Knighton et al., 2017a, b; Georgakakos et al., 2018). Further, in order to understand the sensitivity of this analysis to the *Tp* and *percent impervious* parameters and to establish equifinality, this analysis was repeated twice: 1) by increasing the range of *Tp* to (0, 100) hours (allowing for longer catchment flow paths), and 2) by removing *percent impervious* from the analysis (forcing runoff processes to occur solely as a saturation-excess process (Schneiderman et al., 2007). For information regarding these additional analyses, see the appendix.

3.3 Results and Discussion

3.3.1 Multivariate Regression Analysis of Ecologically Relevant Streamflow Indicators

Outputs of statistical analysis indicate that, while significant relationships exist between the suite of regressors and the hydrologic indices (R-B, BFI, and ETP) (all p-values < 0.001), the three multivariate regressions explain little of data variability (all R^2 values < 0.45). This result suggests an absence of potential additional explanatory variables. Baker et al. (2004) found that watershed size is inversely related to flashiness and while the present results do not establish area

as a statistically significant predictor of R-B at the 95% level, an examination of the data yields a discernable, albeit noisy, trend in agreement (Figure 3).

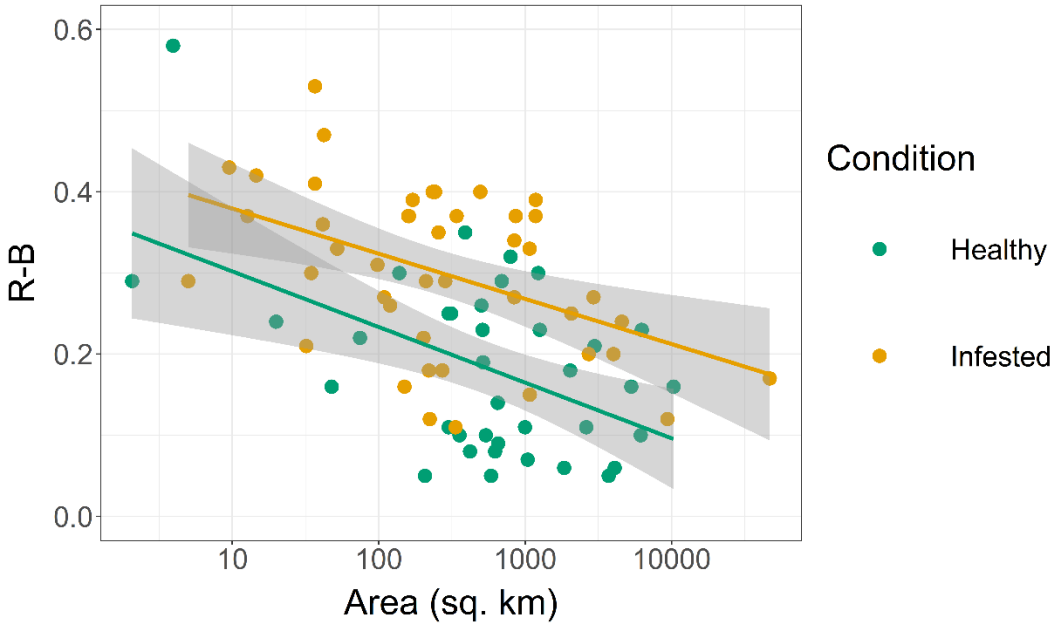

Figure 3*: R-B to Area relationship. Green and yellow lines indicate the best fit linear regressions for healthy and infested catchments, respectively. Shaded area represents the 95% confidence interval on the best-fit linear regression.*

A summary of regression results can be found in Table 3. MAP appears as a significant predictor of R-B and BFI at the 99% and 99.9% levels, respectively, and K_{SAT} is a significant predictor of BFI and ETP at the 99% and 95% levels, respectively. The directionality of relationships between the explanatory and response variables establish that stream flashiness increases and baseflow volumes decrease at higher precipitation levels and the proportion of precipitation removed by ET is greater in locations where soils demonstrate higher saturated hydraulic conductivity and where a higher fraction of total landcover is vegetated. It is noted that none of these relationships appear to be obviously mediated by HWA infestation.

With the exception of the positive relationship between the percentage of total landcover classified as forest and the ETP ratio, which is significant at the 99.9% level, multivariate regression analysis uncovers weak relationships between forest cover, EH condition, and ecologically relevant streamflow characteristics. These outputs of multivariate linear regression are similar to the findings of Tan-Soo et al. (2016), which suggested weak relationships between forest cover and hydrologic characteristics. This analysis, within a purely probabilistic framework, neglects much prior knowledge of the hydrologic functioning of catchments, which could be employed to explain some of the inherent variability between catchments. Although others have demonstrated that new and interesting hypotheses can be developed through statistical modeling-based meta-analysis of hydrologic datasets (e.g., Evaristo and McDonnell, 2017), this approach is possibly too limiting to sufficiently identify a clear signal of change from within the somewhat large variance in the distributions of streamflow characteristics in this case study, in part due to unconstrained geographic factors that may mask the effects of EH influences.

	R-B			BFI			ETP		
Variable	Coefficient	SE	p-value	Coefficient	SE	p-value	Coefficient	SE	p-value
Intercept	0.43018	0.46522	0.35822	-0.094186	0.468275	0.841161	-0.46919	0.42542	0.27370
Condition	-0.29529	0.31344	0.34930	0.064653	0.315502	0.838212	0.32207	0.28616	0.26406
Area	-0.15244	0.09147	0.09992	-0.005878	0.092067	0.949272	-0.02172	0.08696	0.80344
Lat	-0.50790	0.27393	0.06782	0.203333	0.275732	0.463257	0.37539	0.25624	0.14721
ksat	-0.16260	0.09998	0.10825	0.307413	0.100638	0.003158**	0.20156	0.09414	0.03561*
AWC	-0.01603	0.09970	0.87269	0.094967	0.100358	0.347166	0.09591	0.09483	0.31516
MAT	-0.36621	0.23506	0.12363	0.105988	0.236603	0.655528	0.66708	0.21650	0.00295**
MAP	0.36597	0.12027	0.00327**	-0.441265	0.121061	0.000502***	-	-	-
Perc Forest	-0.14485	0.11271	0.20287	-0.016947	0.113449	0.881669	-0.40992	0.10296	0.00016***
Adjusted R^2	0.3659			0.3576			0.4241		
p-value	<0.001			<0.001			<0.001		

,,*** indicate significance at the 95%, 99%, and 99.9% levels, respectively*

***Table 3**: Regression Analysis Descriptive Statistics for all three indices.*

3.3.2 Non-Parametric Test

CDFs of the data generated through the computation of each of the three indices separated by EH condition reveal statistically significant trends in the context of the non-parametric two-sample K-S test (Figure 4). The distribution of infested sites indicates greater stream flashiness, lower baseflow volumes, and possibly higher storm runoff responses to precipitation at these catchments. K-S test p-values of 0.02 and 0.07 suggest HWA are a potentially responsible factor. While less statistically significant, the distribution of data with respect to ETP ratio indicates lower ET volumes at infested sites, which, taken in the context that the dataset, reports higher average forest cover in these locations, may also implicate a disturbance associated with HWA infestation.

3.3.3 Lumped VSA Model Calibration

The 10^{th} percentile, median, and 90^{th} percentile scores across model runs for all sites are 0.15, 0.52, 0.64, respectively. Model performance is best in the Northeastern states (see Figure 5), the region for which JoFlow was developed (Archibald et al., 2014). While the major runoff mechanisms of saturation excess (SE) and Hortonian flow are heterogeneously spatially distributed and often coupled, the Northeastern U.S., characterized by dense vegetation, a humid climate, and higher soil K_{SAT} values relative to the Midwest, exhibits runoff generation dominated by SE processes (Walter et al., 2003; Archibald et al., 2014; Buchanan et al., 2018).

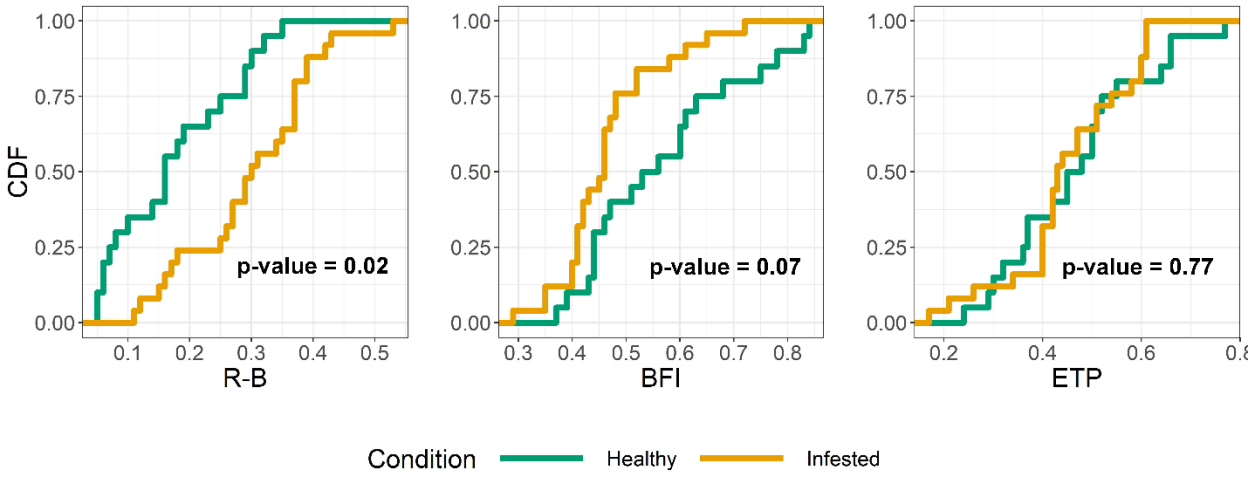

***Figure 4**: CDFs of Hydrologically Relevant Indices by Condition.*

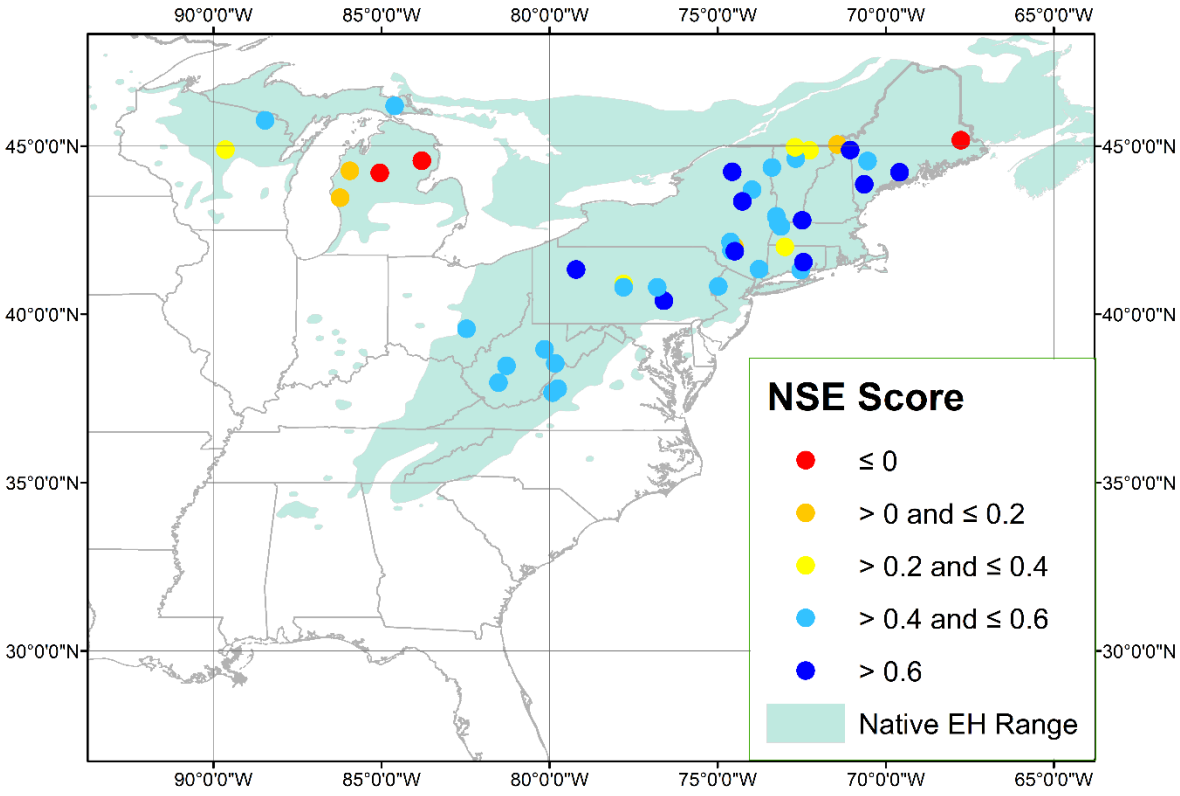

***Figure 5**: Distribution of site NSE scores by geographic location.*

3.3.4 Comparison of Hydrologic Model Parameter Sets and Flow Partitioning

Comparing the CDFs of the fraction of simulated surface runoff to total simulated stream discharge across healthy and infested catchments (Figure 6) reveals that the distribution of infested sites suggests a greater proportion of surface runoff (K-S test p-value = 0.23). This result is generally in agreement with the catchment scale study of Kim et al. (2017). A reduction in stomatal conductance following infestation may yield reduced ET (Domec et al., 2013), increased catchment storage, and increased water yield.

CDFs of hydrologic model parameters for both healthy and infested catchments generated to better understand the mechanism by which EH infestation is controlling the partitioning of catchment water between infiltration and runoff are presented in Figure 7. The baseflow recession coefficient (*rec_coef*) is estimated as significant ($p < 0.05$). This parameter controls the release of catchment-stored water to stream discharge, where lower values indicate longer pathways possibly through groundwater, likely capturing a direct relationship between increased infiltration and forest cover (Lozano-Baez et al., 2019) and representing streams with more sustained baseflows. Infested sites exhibit higher baseflow recession coefficient values, indicating that water moves through shorter flow pathways.

Although not sensitive at the prescribed levels, CDFs of *Se_min, percent impervious*, *PETmax,* and *C1* parameters (see Table 2) subjectively exhibit separation between infested and non-infested sites, which could further indicate process sensitivity.

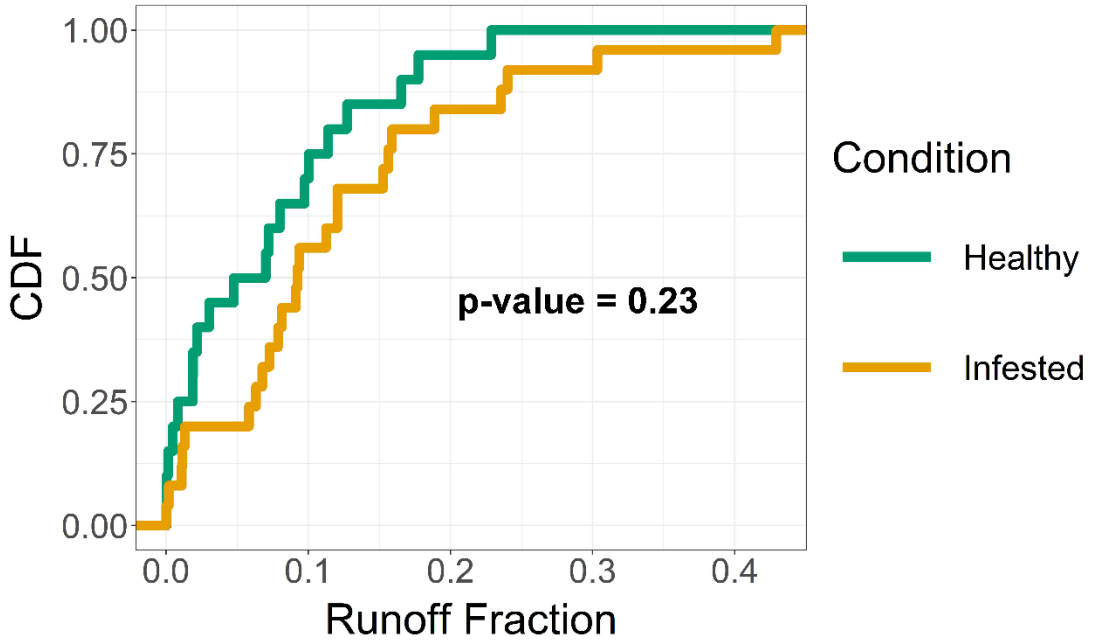

***Figure 6**: CDF plot for Runoff Fraction by Condition.*

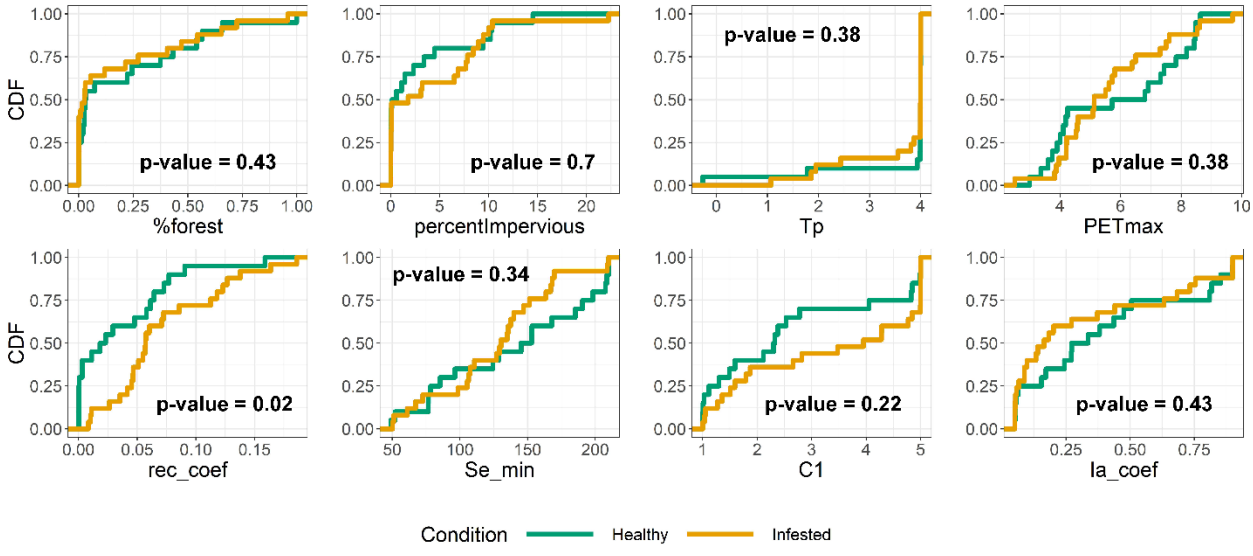

***Figure 7**: CDF plots for all optimal parameter values by Condition.*

The *Se_min* parameter describes the minimum catchment storage on a given day, S_t, through the relationship expressed in Equation 9, where SW_t is daily soil water content (mm). S_t is, in turn, used to determine the storm runoff response, R_t, to precipitation, P (Equation 10) where a smaller S_t value corresponds with a large storm runoff.

$$S_t = Se\_min + C1(AWC - SW_t) \tag{9}$$

$$R_t = \frac{P^2}{P - S_t} \tag{10}$$

The CDFs of *Se_min* demonstrate that healthy EH catchments are more likely to exhibit higher storage and, therefore, reduced stream discharge, especially in the form of storm runoff. This effective catchment storage could be reflective of true changes such as canopy storage provided by EH needles (Guswa and Spence, 2012). The decreased *Se_min* parameter could further be the result of the DDS algorithm attempting to reproduce increased runoff as would occur if the VSA was expanded under reduced catchment transpiration conditions as suggested by Ford and Vose (2007).

The *percent impervious* parameter allows for some portion of catchment precipitation to be converted directly into discharge independent of S_t. Optimal values of this parameter appear to be greater for infested sites near the median of each distribution, which generally reflects increased runoff and may further indicate persistent VSA dilation. The *C1* parameter (Equation 9) describes the slope of the relationship between storage and soil water deficit (AWC – SW) predicated on a modification of the Curve Number (Equation 10) approach following Schneiderman et al. (2007). This parameter controls the sensitivity of surface runoff to

catchment storage and the pertinent CDFs indicate that infested sites have a higher sensitivity relative to healthy sites, assuming SE flow dominated hydrology.

Finally, the *PETmax* parameter demonstrates that discharge at healthy sites is better explained when allowing for higher catchment ET demand, similar to the multivariate regression analysis results. This outcome further agrees with the observations that infested EH stands experience a reduction in stomatal conductance, reduced catchment ET, and higher discharge.

In concert, CDFs of optimal parameter calibrations across the dataset demonstrate, at varying levels of statistical significance, that sites located within HWA range exhibit shorter catchment flow-paths, lower catchment storage, and possibly VSA dilation effects, suggesting more prominent surface runoff responses to precipitation; although the differences were not consistently significant, their systematic patterns are consistent with anticipated impacts of HWA infestation. In particular, these results support trends evinced by CDFs of hydrologic indices generated with the data prior to simulation: catchments within HWA range exhibit higher stream regime flashiness, and lower baseflows and ET rates.

3.3.5 Regional Influence of Eastern Hemlock Infestation on Catchment Hydrology

Non-parametric analysis (Figure 4) and the model informed approach (Figures 6 and 7) identify an influence of HWA infestation on catchment hydrology. CDFs of observed hydrologic indices (Figure 4) suggest that catchments within HWA range experience higher stream regime flashiness, and lower baseflows and ET rates. Note that EH infestation was spatially correlated with lower soil K_{SAT} and AWC (Figure 2), potentially confounding conclusions about the hydrological importance of EH condition. Further, the poleward movement of the HWA yields a

latitudinal gradient of EH infestation (Figure 1), possibly suggesting climate and local weather as an explanation for the differences in hydrologic pathways between the two groupings.

The hydrologic simulation approach allows for control on varied soil properties and climate forcing, yet this methodology still yields evidence of the hydrological consequentiality of HWA infestation. CDFs of optimal hydrologic parameter values (Figure 7) across the dataset demonstrate that sites located within HWA range exhibit shorter flow-path lengths, lower catchment storage, and possibly VSA dilation effects, suggesting more prominent surface runoff reactions to precipitation.

Further, the relationship between infestation and runoff is evidently not significantly related to changes in catchment ET. Both the ETP ratio (Figure 4) and the simulated *PETmax* parameter (Figure 7) do not establish ET as a statistically significant or physically prominent driver of observed bifurcations in hydrologic trends across infested and healthy sites. This result is interesting as previous stand (Brantley et al., 2013; Domec et al., 2013) and catchment-level studies (Kim et al., 2017; Knighton et al., In Review) have identified changes to ET as one of the dominant results of EH infestation and loss.

On the other hand, the calibrated *C1* parameter (Figure 7), which describes VSA hydrology, illustrates that VSA dilation may determine runoff response differences observed across the two catchment groupings. This result indicates that while the reduction in forest ET as a result of EH decline may not necessarily transform precipitation partitioning to the extent of increasing runoff (as in Brantley et al., 2014), reduced canopy interception and increased VSA width could possibly do so (Ford and Vose, 2007). This is further supported by the higher *Se_min* parameter distributions at healthy sites (Figure 7), which apprehend canopy storage effects. The BFI distribution (Figure 4) and the modeled *rec_coef* outputs (Figure 7) also

illuminate differences in catchment storage dynamics along EH condition, with healthy sites feeding a greater proportion of their total stream discharge through sloping groundwater input.

Finally, Buchanan et al. (2018) find that saturation excess overland flow prevails over Hortonian flow generation throughout the Eastern U.S. and the coastal areas around the Great Lakes. That the dominant surface runoff generation process is homogenous and subject to VSA hydrology across the sample region further imputes observed surface runoff differences to VSA effects. Therefore, in order to capture this critical mechanistic detail, it is imperative to utilize a model that numerically describes saturation excess runoff generation, such as JoFlow.

Collectively, the present analyses identify variance in components of infiltration-runoff partitioning between healthy and infested sites, such as baseflow, VSA hydrology, and flow responses to throughfall, as the primary contributors to hydrological differences observed (Stadler et al., 2005; Ford and Vose, 2007). Note that while JoFlow resolves some critical climatological and edaphic factors, it does not account for ecological succession effects, which invariably modulate such partitioning over time. Guswa and Spence (2012), for example, find that while EH canopies intercept a greater volume of precipitation relative to deciduous species, the latter more than account for this difference with higher transpiration.

3.3.6 Statistical Analysis in Hydrology

Recent studies have suggested that we may uncover new and interesting hydrologic insights through statistically-based meta-analysis (e.g., Evaristo and McDonnell, 2017). The research presented considered three methodological approaches for the evaluation of its research questions: 1) a parametric statistical test, 2) a non-parametric statistical test, and 3) comparison

of calibrated hydrologic model parameter values. The parametric statistical test did not identify a convincing influence of EH infestation on several ecologically relevant catchment discharge metrics. In contrast, the non-parametric (K-S test) and the hydrologic modeling-based approaches both suggest a clear influence of HWA infestation on catchment hydrology.

Disagreement among the methodologies employed evinces that certain tests may be better suited for the evaluation of land cover influence on hydrologic partitioning of precipitation into stream discharge and infiltration. The multivariate regressions attempted to control for climate (e.g., MAP, MAT) and land surface variables (e.g., K_{SAT}) that would have some physical influence on catchment hydrology. Yet, their results yielded the insight that regression analysis is perhaps greatly limited by its open-ended framework, in the sense that while it attempts to minimize unexplained variance by identifying linear relationships between regressors and the response variable, it neglects to account for ecohydrological relationships between explanatory variables and catchment discharge, similar to the limitations of the regression analysis in Bradshaw et al. (2007) as described by Van Dijk et al. (2009). Omitting these known physical dynamics from analysis also increases the risk of multicollinearity, which JoFlow avoids through a mechanistic framework of relations between the different variables.

Finally, regression analysis relies on accomplishing a careful balance between the identification of appropriate explanatory variables to provide meaningful results while avoiding indiscriminate parameterization leading to an overdetermined system. It is proposed here that previous studies of forest influence on flooding risk (e.g., Bradshaw et al. 2007; Tan-Soo et al., 2016; Brogna et al. 2017) may not have utilized a holistic methodology.

On the other hand, mechanistic hydrologic models used in concert with probabilistic analysis have provided a clear path towards circumventing some of the challenges of purely

probabilistic analysis. Even where statistical analysis yields general trends in the directionality of relationships between different physical components of catchments, simulation modeling allows the opportunity to elucidate intra-watershed ecohydrological processes driving these relationships. Physically-based models offer a convenient framework to leverage knowledge of well-described physical processes (e.g., mass balance, energy balance of the forest canopy, snowmelt dynamics) and extract additional information contained in the time-order of observations, without over-emphasizing results that may be attributed to autocorrelated observations.

3.4 Broader Impacts

The frequency and intensity of extreme precipitation (EP) and flooding events in the Eastern U.S. have been increasing (DeGaetano, 2009; Kunkel et al., 2013; Armstrong et al., 2014; Frei et al., 2015; Huang et al., 2017), driven by a phase shift of the Atlantic Multidecadal Oscillation and concomitant increases in sea-surface temperatures and the magnitude of tropical cyclones in the region (Huang et al., 2018). Frei et al. (2015) find that both extreme streamflow and EP events, a product of synoptic scale meteorological processes, are increasing in frequency in the warm season (June-October). This joint-trend diverges when considering magnitude, however, with EP events consistently larger in the warm season and extreme streamflow events exhibiting greater intensity in the cold season (November-May). Further, recent regional increases in precipitation, driven primarily by summer and fall season meteorology, can be attributed to few EP events resulting from the increased magnitude of tropical cyclones (Huang et al., 2017, 2018).

These uptrends may produce even greater flooding in regions experiencing ET rate decline and hydrologic regime instability as a result of EH extirpation. While forest transition to deciduous species with higher water use potentials can serve to mitigate EP-related increases in water availability, decreases in leaf-off season ET may promote greater cool season discharge (Daley et al., 2007; Brantley et al., 2013; Knighton et al., In Review). As EH transpires throughout the year, often serving as the primary control on winter and spring season transpiration within its local environment (Ford and Vose, 2007), EH loss can potentially drive higher soil moisture and catchment water yield in these seasons (Stadler et al., 2005; Lustenhouwer et al., 2012; Kim et al. 2017).

Further, HWA infestation has been found to prompt elevated peak-flows following high intensity storm events (Brantley et al., 2014), and EH loss in concert with the increasing magnitude of extreme precipitation events (Frie et al., 2015) may induce greater riverine flooding.

3.5 Conclusions

This chapter investigates the relationship between Eastern hemlock condition and various ecohydrologic factors that determine stream discharge characteristics. Hemlock woolly adelgid presence has expanded throughout much of coastal Eastern and mid-Atlantic U.S., posing a veritable challenge to the continued health of Eastern hemlock stands and possibly transforming the hydrologic and biogeochemical paradigms they modulate. The present research employs a combination of statistical and simulation modeling analyses for increased methodological rigor to evaluate similarities and differences in the outcomes of both approaches.

For a regional-scale dataset of sites across multiple states, a suite of catchments characteristics was regressed over three hydrologic indices to determine whether Hemlock woolly adelgid presence predicts trends in stream flashiness, baseflow, or catchment evapotranspiration. While multivariate regression results did not identify infestation as a statistically significant explanatory variable, non-parametric analysis of cumulative distribution functions generated with the data suggest that catchments within hemlock woolly adelgid range exhibit higher flashiness (K-S test p-value < 0.05) and lower baseflows (K-S test p-value < 0.1). Statistical analysis outcomes of this work shared indeterminacy with other meta-analyses examining the relationship between land cover characteristics and hydrologic regime (e.g., Bradshaw et al., 2007; Tan-Soo et al., 2016; Brogna et al., 2017), potentially indicating that a purely statistical methodology may not capture dynamic physical ecohydrologic relationships.

Catchment data for a subset of the total sample were then utilized to parameterize a physically-based model and optimal values for additional calibration parameters were determined to further characterize each site. Modeling outcomes suggest that sites within hemlock woolly adelgid range exhibit shorter flow pathways and likely lower baseflows (K-S test p-value < 0.05); lower catchment storage and higher sensitivity of storage to soil water deficit, reduced maximum potential evapotranspiration, and increased surface runoff (K-S test p-values < 0.5).

Through a coarse regional scale analysis, this research finds that hemlock woolly adelgid presence modifies a number of ecohydrological characteristics and precipitation partitioning between groundwater flows and surface runoff, and that a semi-physically based simulation illuminates trends not captured by a simple regression analysis.

CHAPTER 4

FUTURE RESEARCH

It is important to note here that while this study supports the thesis that EH mortality will be succeeded in the immediate term by an increase in fluvial flooding potential, it favors an expanded spatial scale above a refined understanding of species-specific attributes of EH and potential successional species with regards to hydrologic control. In a sense, the research presented in this thesis relied on the law of large numbers, illuminating those physical relationships in nature that may mediate the link between EH loss and hydrologic regime transformations that pervade across a regional sample. This chapter presents brief summaries of two additional studies proposed as an extension of the research reported in this thesis. This future work will serve to:

1. Supplement current understanding of the plant hydraulics of EH and candidate successional species.
2. Investigate changes in flooding regime across a catchment and New York state scale in both the immediate term after EH extirpation, and following ecological succession. This work will integrate a more specific understanding of plant hydraulics in its ecohydrologic modeling component.

4.1 Stable Water Isotope Fractionation During Plant Water Uptake and Isotope Mixing During Water Storage

It is established that the isotopic composition of water within plant leaves is distinct from that of the surrounding water vapor in the air. This is due to the low vapor pressure of water constituted by heavy stable water isotopes Oxygen-18 (^{18}O) and Deuterium (^{2}H) (heavy water) and the lower diffusivity of heavy water with air, relative to the most common water molecule $^{1}H_2{}^{16}O$ (light water). Transpiration, therefore, fractionates water at the leaf-air interface, enriching leaf water with respect to heavy isotopes and depleting water vapor in the air surrounding (Farquhar et al., 2006). It is unclear whether a similar fractionation occurs at the root-soil interface. Early studies advancing this theme of inquiry found no evidence for this process (e.g., Flanagan and Ehleringer, 1991). More recently, Oerter et al. (2019) demonstrated isotopic similarity between soil water and the xylem water of streamside trees. However, hydrogen isotope fractionation has been identified at the roots of halophytic and xerophytic plants (Ellsworth et al., 2007). Further, Barbeta et al. (2018) observe a positive relationship between transpiration rate, soil water content, and soil ^{2}H enrichment, suggesting that at least in the case of European beech (*Fagus sylvatica*), a temperate deciduous species, fractionation occurs during plant water uptake. This is an open area of research and it is conceivable that a similar process occurs in the case of EH, but no known studies have actively explored this thesis. Precisely understanding processes that may transform isotopic signatures during transpiration, such as root-level fractionation and isotopic mixing within the plant, is critical to accurately simulate plant hydraulic control of fluvial flooding. In the absence of this understanding, it is possible to misinterpret differences or

similarities in soil, xylem, and leaf water with regards to plant root plasticity and water uptake depth.

A future study is proposed to investigate isotopic fractionation and mixing within EH, American beech (*Fagus grandifolia*) (AB), and Black birch (*Betula lenta*) (BB). Saplings of these three species will be grown in soil plugs within a controlled environment, with adjustable vapor pressure deficit, temperature, and photoperiod, and provided water with a known baseline isotopic composition. Isotopic signatures within the soil, roots, leaves, and at different segments along the stem length will be closely monitored under different climatological conditions. Deviations of root, stem, and leaf water $\delta^{18}O$ and $\delta^{2}H$ from the local meteoric water line will be measured and plotted to evaluate fractionation. Further, $\delta^{18}O$ and $\delta^{2}H$ measured at each stem length will be plotted against stem height to determine internal isotopic mixing. Determining whether the EcH2O-iso simulations carried out for the study outlined in the next section should assume no isotope mixing, plug-flow, or complete mixing, and whether they should account for root-soil interface fractionation will enhance the veracity of modeling work.

4.2 Shifts in Fluvial Flood Regimes Following Eastern Hemlock Loss and Ecological Succession

It is expected that riverine flooding will increase throughout the U.S. as the Earth's surface temperature continues to rise over the next 20-30 years (Willner et al., 2018). The increasing frequency and magnitude of extreme precipitation events in the Northeastern U.S. (e.g., Frei et al., 2015; Huang et al., 2017), and the loss of forest cover-based catchment water storage, such as through the extirpation of EH, are likely to intersect and further drive fluvial flooding risk (see

Chapter 3). Purely statistical models of the relationship between landcover and flooding (e.g., Bradshaw et al., 2007) have arguably exhibited oversimplification and misapprehension of physical ecohydrological relationships, and simulation models that elucidate physical processes generating flooding may offer a solution (see Rogger et al., 2017 and Chapter 3). Even so, land surface models generally represent flooding in terms of soil runoff-infiltration partitioning, generalizing plant hydraulics along taxonomic boundaries rather than species-specific functional attributes modulated by environmental factors (Matheny et al., 2017; Knighton et al., In Review). Further, previous research examining the hydrological consequences of EH mortality have relied primarily on measurements of stomatal conductance and ET (Brantley et al., 2013; Domec et al., 2013) or canopy interception and storage (Stadler et al., 2005; Ford and Vose, 2007; Guswa and Spence, 2012), often omitting the role of root water uptake. Yet, comparisons of the isotopic signatures of xylem water sourced from EH and AB and soil water indicate that the former species exercises greater groundwater uptake through all seasons, potentially increasing catchment water storage and managing flooding risk (Knighton et al., In Review). In addition, conceptualizations of water uptake have increasingly integrated considerations of root plasticity and the vertical and horizontal heterogeneity of rooting structure (e.g., Fan et al., 2017; Brinkmann et al., 2018).

A set of future studies are proposed here to investigate short-term hydrologic consequences of EH mortality and long-term hydrological regime readjustments effects of succession by AB, BB, or some variable combinations of these two species. More broadly, simulations carried out as a part of these studies will incorporate species-specific plant water uptake data to assess the benefits of incorporating plant hydraulic function in hydrologic modeling. Field-work will be carried out at a long-term hydrologic research catchment located in

Hammond Hill, New York. Sap flux of all three species of interest, as well as shallow soil water content, will be measured through one growing season. Stable water isotope signatures (^{2}H and ^{18}O) of soil and tree xylem water will be analyzed. In the first of this set of papers, field observations will be utilized to calibrate the EcH2O-iso model (Kuppel et al., 2018), and hydrologic simulations of the various scenarios described above will be carried out at a catchment scale. EcH2O-iso is a spatially distributed, physically based ecohydrological model with the capability of tracking stable water isotope tracers and water age. Finally, results from this study will be used to parameterize a regional hydrologic land surface model to understand how the loss of EH could impact flooding across the state of New York.

REFERENCES

Adams, H.D., Luce, C.H., Breshears, D.D., Allen, C.D., Weiler, M., Hale, V.C., Smith, A.M.S., and Huxman, T.E. (2012), Ecohydrological consequences of drought- and infestation-triggered tree die-off: Insights and hypotheses, Ecohydrology, 5(2), 145–159.

Albani, M., Moorcroft, P.R., Ellison, A.M., Orwig, D.A., and Foster, D.R. (2010), Predicting the impact of hemlock woolly adelgid on carbon dynamics of eastern United States forests, Canadian Journal of Forest Research, 40(1), 119–133.

Allen, C.D., Macalady, A.K., Chenchouni, H., Bachelet, D., Mcdowell, N., Vennetier, M., . . . Cobb, N. (2010). A global overview of drought and heat-induced tree mortality reveals emerging climate change risks for forests. Forest Ecology and Management, 259(4), 660-684.

Anderson, J.R., Hardy, E.E., Roach, J.T., & Witmer, R.E. (1976). A land use and land cover classification system for use with remote sensor data. Professional Paper. doi:10.3133/pp964

Archibald, J., Buchanan, B., Fuka, D., Georgakakos, C., Lyon, S., and Walter, M.T. (2014). A simple, regionally parameterized model for predicting nonpoint source areas in the northeastern US. Journal of Hydrology: Regional Studies, 1, 74–92.

Armstrong, W.H., Collins, M.J., and Snyder, N.P. (2014). Hydroclimatic flood trends in the northeastern United States and linkages with large-scale atmospheric circulation patterns. Hydrological Sciences Journal, 59, 1636–1655.

Baker, D.B., Richards, R.P., Loftus, T.T., and Kramer, J.W. (2004). A New Flashiness Index: Characteristics and applications to midwestern rivers and streams. Journal of the American Water Resources Association, 40(2), 503-522.

Barbeta, A., Gimeno, T., Clave, L., Jones, S., Wingate, L., Frejaville, B., and Ogee, J. (2018). Fractionation of δ2H during root water uptake is linked to plant transpiration in saplings of a temperate tree species. American Geophysical Union, Fall Meeting 2018, Abstract #H22H-04.

Bearup, L.A., Maxwell, R.M., Clow, D.W., and Mccray, J.E. (2014). Hydrological effects of forest transpiration loss in bark beetle-impacted watersheds. Nature Climate Change, 4(6), 481-486.

Bond, B.J., Menzier, F.C., and Brooks, J.R. How trees influence the hydrological cycle in forest ecosystems In: Hydroecology and ecohydrology: Past, present and future (p. 7-35). Chichester, West Sussex, England: John Wiley & Sons.

Bosch, J., and Hewlett, J. (1982). A review of catchment experiments to determine the effect of vegetation changes on water yield and evapotranspiration. Journal of Hydrology, 55(1-4), 3-23.

Bradshaw, C.J., Sodhi, N.S., PEH, K.S.H., and Brook, B.W. (2007). Global evidence that deforestation amplifies flood risk and severity in the developing world. Global Change Biology, 13(11), 2379-2395.

Brantley, S., Ford, C.R., and Vose, J.M. (2013). Future species composition will affect forest water use after loss of eastern hemlock from southern Appalachian forests. Ecological Applications, 23(4), 777-790.

Brantley, S.T., Miniat, C.F., Elliott, K.J., Laseter, S.H., and Vose, J.M. (2014). Changes to southern Appalachian water yield and stormflow after loss of a foundation species. Ecohydrology, 8(3), 518-528.

Brantley, S.L., Eissenstat, D.M., Marshall, J.A., Godsey, S.E., Balogh-Brunstad, Z., Karwan, D.L., ..., and Chadwick, O. (2017). Reviews and syntheses: On the roles trees play in building and plumbing the critical zone. Biogeosciences (Online), 14(22).

Brinkmann, N., Eugster, W., Buchmann, N., and Kahmen, A. (2018). Species specific differences in water uptake depth of mature temperate trees vary with water availability in the soil. Plant Biology, 21(1), 71-81.

Brogna, D., Vincke, C., Brostaux, Y., Soyeurt, H., Dufrêne, M., and Dendoncker, N. (2017). How does forest cover impact water flows and ecosystem services? Insights from "real-life" catchments in Wallonia (Belgium). Ecological Indicators, 72, 675-685.

Brown, A.E., Zhang, L., Mcmahon, T.A., Western, A.W., and Vertessy, R.A. (2005). A review of paired catchment studies for determining changes in water yield resulting from alterations in vegetation. Journal of Hydrology, 310(1-4), 28-61.

Buchanan, B., Auerbach , D.A., Knighton, J.O., Evensen, D., Fuka, D.R., Easton , Z.M., Wieczorek, M., Archibald, J.A., McWilliams, B., and Walter, M.T. 2018. Estimating dominant runoff modes across the conterminous United States. Hydrological Processes, 32(26), 3881-3890.

Catovsky, S., Holbrook, N.M., and Bazzaz, F.A. (2002). Coupling whole-tree transpiration and canopy photosynthesis in coniferous and broad-leaved tree species. Canadian Journal of Forest Research, 32(2), 295-309.

Cessna, J.F., and Nielsen, C. (2012). Influences of hemlock woolly adelgid–induced stand-level mortality on nitrogen cycling and stream water nitrogen concentrations in Southern Pennsylvania. Castanea, 77(2), 127-135.

Chen, M., Shi, W., Xie, P., Silva, V.B.S., Kousky, V.E., Higgins, R.W., and Janowiak, J.E. (2008), Assessing objective techniques for gauge-based analyses of global daily precipitation. Journal of Geophysical Research: Atmospheres, 113, D4.

Daley, M.J., Phillips, N.G., Pettijohn, C., and Hadley, J.L. (2007). Water use by eastern hemlock (*Tsuga canadensis*) and black birch (*Betula lenta*): implications of effects of the hemlock woolly adelgid. Canadian Journal of Forest Research, 37(10), 2031-2040.

Davis, J.B. 2008. Quantifying the decline in transpiration of *Tsuga canadensis* and predicting water budget implications of succession in southern Appalachian forests. Highlands Biological Station. 8-22 p.

Dingman, S.L. (2002). Physical hydrology. Long Grove, IL: Waveland Press.

Degaetano, A.T. (2009). Time-dependent changes in extreme-precipitation return-period amounts in the continental United States. Journal of Applied Meteorology and Climatology, 48(10), 2086-2099.

Domec, J.C., Rivera, L.N., King, J.S., Peszlen, I., Hain, F., Smith, B., and Frampton, J. (2013). Hemlock woolly adelgid (*Adelges tsugae*) infestation affects water and carbon relations of eastern hemlock (*Tsuga canadensis*) and Carolina hemlock (*Tsuga caroliniana*). New Phytologist, 199(2), 452-463.

Eagleson, P.S. (2002). Ecohydrology: Darwinian expression of vegetation form and function. Cambridge: Cambridge University Press.

Eamus, D., Hatton, T., Cook, P., and Colvin, C. (2006). Ecohydrology: Vegetation Function, Water and Resource Management. Melbourne: CSIRO Publishing.

Eckhardt, K. (2008). A comparison of baseflow indices, which were calculated with seven different baseflow separation methods. Journal of Hydrology, 352(1-2), 168-173.

Ellison, A.M., Bank, M.S., Clinton, B.D., Colburn, E.A., Elliott, K., Ford, C.R., Foster, D.R., Kloeppel, B.D., and Knoepp, J.D. (2005). "Loss of foundation species: Consequences for the structure and dynamics of forested ecosystems". Frontiers in Ecology and the Environment, 3(9), 479.

Ellsworth, P.Z., and Williams, D.G. (2007). Hydrogen isotope fractionation during water uptake by woody xerophytes. Plant and Soil, 291(1-2), 93-107.

Eschtruth, A.K., Cleavitt, N.L., Battles, J.J., Evans, R.A., and Fahey, T.J. (2006). Vegetation dynamics in declining eastern hemlock stands: 9 years of forest response to hemlock woolly adelgid infestation. Canadian Journal of Forest Research, 36(6), 1435-1450.

Evaristo, J., and McDonnell, J.J. (2017). Prevalence and magnitude of groundwater use by vegetation: A global stable isotope meta-analysis. Scientific Reports, 7, 44110.

Ewers, B.E., Gower, S.T., Bond-Lamberty, B., and Wang, C.K. (2005). Effects of stand age and tree species on canopy transpiration and average stomatal conductance of boreal forests. Plant, Cell and Environment, 28(5), 660-678.

Fan, Y., Miguez-Macho, G., Jobbágy, E.G., Jackson, R.B., and Otero-Casal, C. (2017). Hydrologic regulation of plant rooting depth. Proceedings of the National Academy of Sciences, 201712381.

Farquhar, G.D., Cernusak, L.A., and Barnes, B. (2006). Heavy water fractionation during transpiration. Plant Physiology, 143(1), 11-18.

Flanagan, L.B., and Ehleringer, J.R. (1991). Stable isotope composition of stem and leaf water: Applications to the study of plant water use. Functional Ecology, 5(2), 270.

Ford, C.R., and Vose, J.M. (2007). *Tsuga canadensis* (L.) Carr. mortality will impact hydrologic processes in southern Appalachian forest ecosystems. Ecological Applications, 17(4), 1156-1167.

Ford, C.R., Elliott, K.J., Clinton, B.D., Kloeppel, B.D., and Vose, J.M. (2011). Forest dynamics following eastern hemlock mortality in the southern Appalachians. Oikos, 121(4), 523-536.

Frei, A., Kunkel, K.E., and Matonse, A. (2015). The seasonal nature of extreme hydrological events in the northeastern United States. Journal of Hydrometeorology, 16(5), 2065-2085.

Fuka D.R., Walter M.T., Archibald J.A., Steenhuis T.S., and Easton Z.M. (2018). A community based modeling foundation for Eco-Hydrology. Package 'EcohydRology' Version 0.4.12.1. [Available online at https://cran.r-project.org/web/packages/EcoHydRology/EcoHydRology.pdf].

Georgakakos, C.B., Morris, C.K., and Walter, M.T. (2018). Challenges and opportunities with on-farm research: Total and soluble reactive stream phosphorus before and after implementation of a cattle-exclusion, riparian buffer. Frontiers in Environmental Science, 6 (Online).

Gonda-King, L., Gómez, S., Martin, J.L., Orians, C. M., and Preisser, E. L. (2014). Tree responses to an invasive sap-feeding insect. Plant Ecology, 215(3), 297-304.

Gordon, W.S., and Huxman, T.E. Ecohydrology and climate change. In: Hydroecology and ecohydrology: Past, present and future (p. 113-128). Chichester, West Sussex, England: John Wiley & Sons.

Guswa, A.J., and Spence, C.M. (2012). Effect of throughfall variability on recharge: application to hemlock and deciduous forests in western Massachusetts. Ecohydrology, 5(5), 563-574.

Hadley, J.L., Kuzeja, P.S., Daley, M.J., Phillips, N.G., Mulcahy, T., and Singh, S. (2008). Water use and carbon exchange of red oak- and eastern hemlock-dominated forests in the northeastern USA: Implications for ecosystem-level effects of hemlock woolly adelgid. Tree Physiology, 28(4), 615-627.

Hibbert, A.R., and Troendle, C.A. (1988). Streamflow generation by variable source area. In: Forest hydrology and ecology at Coweeta (p. 111-127). New York: Springer-Verlag.

Homer, C.G., Dewitz, J.A., Yang, L., Jin, S., Danielson, P., Xian, G., Coulston, J., Herold, N.D., Wickham, J.D., and Megown, K., 2015, Completion of the 2011 National Land Cover Database for the conterminous United States-Representing a decade of land cover change information. Photogrammetric Engineering and Remote Sensing, 81(5), 345-354.

Hornberger, G.M., Wiberg, P.L., Raffensperger, J.P., and D'Odorico, P. (2014). Elements of physical hydrology. Baltimore: Johns Hopkins University Press.

Hornberger, G.M., and Spear, R.C. (1981). An approach to the preliminary analysis of environmental systems. Journal of Environmental Management, 12, 7-18.

Horton, R.E. (1933). The role of infiltration in the hydrologic cycle. Transactions, American Geophysical Union, 14(1), 446.

Huang, H., Winter, J.M., and Osterberg, E.C. (2018). Mechanisms of abrupt extreme precipitation change over the Northeastern United States. Journal of Geophysical Research: Atmospheres, 123(14), 7179-7192.

Huang, H., Winter, J.M., Osterberg, E.C., Horton, R.M., and Beckage, B. (2017). Total and extreme precipitation changes over the Northeastern United States. Journal of Hydrometeorology, 18(6), 1783-1798.

Jenkins, J.C., Aber, J.D., and Canham, C.D. (1999). Hemlock woolly adelgid impacts on community structure and N cycling rates in eastern hemlock forests. Canadian Journal of Forest Research, 29(5), 630-645.

Kim, J., Hwang, T., Schaaf, C.L., Orwig, D.A., Boose, E., and Munger, J.W. (2017). Increased water yield due to the hemlock woolly adelgid infestation in New England. Geophysical Research Letters, 44(5), 2327-2335.

Kramer, P.J., and Kozlowski, T.T. (1979). Physiology of wood plants. Orlando, FL: Academic Press.

Kunkel, K.E. (2013). Monitoring and understanding changes in extreme storms: State of knowledge. Bulletin of the American Meteorological Society, 94, 499–514.

Kuppel, S., Tetzlaff, D., Maneta, M.P., and Soulsby, C. (2018). EcH2O-iso 1.0: Water isotopes and age tracking in a process-based,distributed ecohydrological model. Geoscientific Model Development Discussions, 1-38.

Knighton, J., Steinschneider, S., and Walter, M.T. (2017a). A vulnerability based, bottom up assessment of future riverine flood risk using a modified peaks over threshold approach and a physically based hydrologic model. Water Resources Research, 53(12), 10043-10064.

Knighton, J., Saia, S.M., Morris, C.K., Archiblad, J.A., and Walter, M.T. (2017b). Ecohydrologic considerations for modeling of stable water isotopes in a small intermittent watershed. Hydrological Processes, 31(13), 2438-2452.

Knighton J., Coneelly, J., and Walter, M.T. In Review. Possible increases in flood frequency due to the loss of Eastern Hemlock in the northeastern US: Observational insights and predicted impacts. Water Resources Research.

Lemordant, L., Gentine, P., Swann, A.S., Cook, B.I., and Scheff, J. (2018). Critical impact of vegetation physiology on the continental hydrologic cycle in response to increasing CO2. Proceedings of the National Academy of Sciences, 115(16), 4093-4098.

Li, C.J., Chai, Y.Q., Yang, L.S., and Li, H.R. (2016). Spatio-temporal distribution of flood disasters and analysis of influencing factors in Africa. Natural Hazards, 82(1), 721-731.

Little, Elbert L., Jr. 1971. Atlas of United States trees. Volume 1. Conifers and important hardwoods. Miscellaneous Publication 1146. Washington, DC: U.S. Department of Agriculture, Forest Service. 9 p., illus. [313 maps, folio]. [Map layer available online at https://www.arcgis.com/home/item.html?id=1d0d5889349849a88a8f645082a7e049].

Loucks, D.P., Beek, E.V., Stedinger, J.R., Dijkman, J.P., and Villars, M.T. (2017). Water resource systems planning and management: An introduction to methods, models, and applications. Cham, Switzerland: Springer.

Lovett, G.M., Weathers, K.C., Arthur, M.A., and Schultz, J.C. (2004). Nitrogen cycling in a northern hardwood forest: Do species matter? Biogeochemistry, 67(3), 289-308.

Lozano-Baez, S.E., Cooper, M., Meli, P., Ferraz, S.F., Rodrigues, R.R., and Sauer, T.J. (2019). Land restoration by tree planting in the tropics and subtropics improves soil infiltration, but some critical gaps still hinder conclusive results. Forest Ecology and Management, 444, 89-95.

Lustenhouwer, M.N., Nicoll, L., and Ellison, A.M. (2012). Microclimatic effects of the loss of a foundation species from New England forests. Ecosphere, 3(3).

Matheny, A.M., Mirfenderesgi, G., and Bohrer, G. (2017). Trait-based representation of hydrological functional properties of plants in weather and ecosystem models. Plant Diversity, 39(1), 1-12.

Mcdowell, N., Pockman, W.T., Allen, C.D., Breshears, D.D., Cobb, N., Kolb, T., …, and Yepez, E.A. (2008). Mechanisms of plant survival and mortality during drought: Why do some plants survive while others succumb to drought? New Phytologist, 178(4), 719-739.

Meinzer, F.C., James, S.A., and Goldstein, G. (2004). Dynamics of transpiration, sap flow and use of stored water in tropical forest canopy trees. Tree Physiology, 24(8), 901-909.

Mladenoff, D.J. (1987). Dynamics of nitrogen mineralization and nitrification in hemlock and hardwood treefall gaps. Ecology, 68(5), 1171-1180.

Moore, G.W., Bond, B.J., Jones, J.A., Phillips, N., and Meinzer, F.C. (2004). Structural and compositional controls on transpiration in 40- and 450-year-old riparian forests in western Oregon, USA. Tree Physiology, 24(5), 481-491.

Nash, J., and Sutcliffe, J. (1970). River flow forecasting through conceptual models part I — A discussion of principles. Journal of Hydrology, 10(3), 282-290.

Nathan, R.J. and McMahon, T.A. (1990). "Evaluation of automated techniques for base flow and recession analysis." Water Resources Research 26(7): 1465-1473.

Ogden, F.L. and Watts, B.A. (2000). Saturated area formation on nonconvergent hillslope topography with shallow soils: A numerical investigation. Water Resources Research, 36 (7), 1795-1804.

Oerter, E.J., Siebert, G., Bowling, D.R., and Bowen, G. (2019). Soil water vapour isotopes identify missing water source for streamside trees. Ecohydrology, e2083 (Online).

Orwig, D.A., Cobb, R.C., D'Amato, A.W., Kizlinski, M.L., and Foster, D.R. (2008). Multi-year ecosystem response to hemlock woolly adelgid infestation in southern New England forests. Canadian Journal of Forest Research, 38(4), 834-843.

Orwig, D.A., and Foster, D.R. (1998). Forest response to the introduced hemlock woolly adelgid in Southern New England, USA. Journal of the Torrey Botanical Society, 125(1), 60.

Pataki, D., and Oren, R. (2003). Species differences in stomatal control of water loss at the canopy scale in a mature bottomland deciduous forest. Advances in Water Resources, 26(12), 1267-1278.

Philip, J.R. (1966). Plant water relations: Some physical aspects. Annual Review of Plant Physiology, 17(1), 245-268.

Priestley, C.H., and Taylor, R.J. (1972). On the assessment of surface heat flux and evaporation using large-scale parameters. Monthly Weather Review, 100(2), 81-92.

Raffa, K.F., Aukema, B.H., Bentz, B.J., Carroll, A.L., Hicke, J.A., Turner, M.G., and Romme, W.H. (2008). Cross-scale drivers of natural disturbances prone to anthropogenic amplification: The dynamics of bark beetle eruptions. BioScience, 58(6), 501-517.

Roberts, S.W., Tankersley, R., and Orvis, K.H. (2009). Assessing the potential impacts to riparian ecosystems resulting from hemlock mortality in Great Smoky Mountains National Park. Environmental Management, 44(2), 335-345.

Rodriguez-Iturbe, I., Porporato, A., Laio, F., and Ridolfi, L. (2001). Plants in water-controlled ecosystems: Active role in hydrologic processes and response to water stress. Advances in Water Resources, 24(7), 695-705.

Rogger, M., Agnoletti, M., Alaoui, A., Bathurst, J.C., Bodner, G., Borga, M., ..., and Holden, J. (2017). Land use change impacts on floods at the catchment scale: Challenges and opportunities for future research. Water resources research, 53(7), 5209-5219.

Royer, P.D., Breshears, D.D., Zou, C.B., Villegas, J.C., Cobb, N.S., and Kurc, S.A. (2012). Density-dependent ecohydrological effects of Piñon–Juniper woody canopy cover on soil microclimate and potential soil evaporation. Rangeland Ecology and Management, 65(1), 11-20.

Sauer, V.B., and Turnipseed, D.P. (2010). Stage measurement at gaging stations: U.S. Geological Survey Techniques and Methods, Book 3, Section A, (Available at http://pubs.usgs.gov/tm/tm3-a7/).

Schneiderman, E.M., Steenhuis, T.S., Thongs, D.J., Easton, Z.M., Zion, M.S., Neal, A.L., ..., and Walter, M.T. (2007). Incorporating variable source area hydrology into a curve-number-based watershed model. Hydrological Processes, 21(25), 3420-3430.

Schume, H., Jost, G., and Hager, H. (2004). Soil water depletion and recharge patterns in mixed and pure forest stands of European beech and Norway spruce. Journal of Hydrology, 289(1-4), 258-274.

Siderhurst, L.A., Griscom, H.P., Hudy, M., and Bortolot, Z.J. (2010). Changes in light levels and stream temperatures with loss of eastern hemlock (*Tsuga canadensis*) at a southern Appalachian stream: Implications for brook trout. Forest Ecology and Management, 260(10), 1677-1688.

Snyder, C.D., Young, J.A., Lemarié, D.P., and Smith, D.R. (2002). Influence of eastern hemlock (*Tsuga canadensis*) forests on aquatic invertebrate assemblages in headwater streams. Canadian Journal of Fisheries and Aquatic Sciences, 59(2), 262-275.

Soil Survey Staff, Natural Resources Conservation Service, United States Department of Agriculture. Web Soil Survey. Available online at https://websoilsurvey.nrcs.usda.gov/. Accessed 2018.

Sprenger, M., Leistert, H., Gimbel, K., and Weiler, M. (2016). Illuminating hydrological processes at the soil-vegetation-atmosphere interface with water stable isotopes. Reviews of Geophysics, 54(3), 674-704.

Stadler, B., Müller, T., Orwig, D., and Cobb, R. (2005). Hemlock woolly adelgid in New England forests: Canopy impacts transforming ecosystem processes and landscapes. Ecosystems, 8(3), 233-247.

Stednick, J.D. (1996). Monitoring the effects of timber harvest on annual water yield. Journal of Hydrology, 176(1-4), 79-95.

Steenhuis, T., and Molen, W.V. (1986). The Thornthwaite-Mather procedure as a simple engineering method to predict recharge. Journal of Hydrology, 84(3-4), 221-229.

Swank, W. T., Swift, L.W., and Douglas, J.E. (1988). Streamflow changes associated with forest cutting, species conversions, and natural disturbances. In: Forest hydrology and ecology at Coweeta (p. 297-312). New York: Springer-Verlag.

Swift, L.W., Swank, W.T., Mankin, J.B., Luxmoore, R.J., and Goldstein, R.A. (1975). Simulation of evapotranspiration and drainage from mature and clear-cut deciduous forests and young pine plantation. Water Resources Research, 11, 667-673.

Tan-Soo, J.S., Adnan, N., Ahmad, I., Pattanayak, S.K., and Vincent, J.R. (2016). Econometric evidence on forest ecosystem services: deforestation and flooding in Malaysia. Environmental and Resource Economics, 63(1), 25-44.

Thornthwaite, C.W. and J.R. Mather, 1955. The water balance. Laboratory of Climatology, No. 8, Centerton, N.J.

Thornthwaite, C.W. (1948). An approach toward a rational classification of climate. Soil Science, 66(1), 77.

Tolson, B.A., and Shoemaker, C.A. (2007). Dynamically dimensioned search algorithm for computationally efficient watershed model calibration. Water Resources Research, 43(1), W01413.

USDA Forest Service. (2018). Distribution of HWA in 2017 [Map]. [Available online at http://hiro.ento.vt.edu/hwa/index.php/distribution-maps/].

USGS, 2018: USGS Water Data for the Nation. Accessed 11-21 March 2018. [Available online at http://waterdata.usgs. gov/nwis/].

Van Dijk, A.I., Van Noordwijk, M., Calder, I.R., Bruijnzeel, S.L., Schellekens, J.A.A.P., and Chappell, N.A. (2009). Forest–flood relation still tenuous–comment on 'Global evidence that deforestation amplifies flood risk and severity in the developing world' by C.J.A. Bradshaw, N.S. Sodi, K.S.H. Peh, and B.W. Brook. Global Change Biology, 15(1), 110-115.

Villarini, G., Mandapaka, P.V., Krajewski, W.F., and Moore, R.J. (2008). Rainfall and sampling uncertainties: A rain gauge perspective. Journal of Geophysical Research, 113, D11.

Walter, M.T., Mehta, V.K., Marrone, A.M., Boll, J., Gérard-Marchant, P., Steenhuis, T.S., and Walter, M.F. (2003). Simple Estimation of Prevalence of Hortonian Flow in New York City Watersheds. Journal of Hydrologic Engineering, 8(4), 214-218.

Walter, M.T., Brooks, E.S., Mccool, D.K., King, L.G., Molnau, M., and Boll, J. (2005). Process-based snowmelt modeling: Does it require more input data than temperature-index modeling? Journal of Hydrology, 300(1-4), 65-75.

Wang, K., and Dickinson, R.E. (2012). A review of global terrestrial evapotranspiration: Observation, modeling, climatology, and climatic variability. Reviews of Geophysics, 50(2), RG2005.

Willner, S.N., Levermann, A., Zhao, F., and Frieler, K. (2018). Adaptation required to preserve future high-end river flood risk at present levels. Science Advances, 4(1), eaao1914.

Winter, T.C. (1981). Uncertainties in estimating the water balance of lakes. Journal of the American Water Resources Association, 17(1), 82-115.

Wood, P.J., Hannah, D.M., and Sadler, J.P. (2008a). Ecohydrology and hydroecology: An introduction. In: aHydroecology and ecohydrology: Past, present and future (p. 1-6). Chichester, West Sussex, England: John Wiley & Sons.

Wood, P.J., Hannah, D.M., and Sadler, J.P. (2008b). Hydroecology and ecohydrology: Past, present and future. Chichester, West Sussex, England: John Wiley & Sons.

Yorks, T.E., Jenkins, J.C., Leopold, D.J., Raynal, D.J., Orwig, D.A. (2000). Influences of eastern hemlock mortality on nutrient cycling. In: McManus, K.A., Shields, K.S., Souto, D.R., eds. Proceedings: Symposium on sustainable management of hemlock ecosystems in eastern North America. Gen. Tech. Rep. NE-267. Newtown Square, PA: U.S. Department of Agriculture, Forest Service, Northeastern Forest Experiment Station. 126-133.

Young, R.F., Shields, K.S., and Berlyn, G.P. (1995). Hemlock woolly adelgid (Homoptera: Adelgidae): Stylet bundle insertion and feeding sites. Annals of the Entomological Society of America, 88(6), 827-835.

APPENDIX

SUPPLEMENTARY ANALYSIS

Two additional simulation analyses were carried out to explore cross-parameter sensitivity and alternative parameterizations that may improve model performance across the sample, and to establish equifinality in research findings. In both cases, the prior methodology of calibrating JoFlow to each catchment using the DDS algorithm and preserving the calibration parameter set that maximizes model NSE score following 10,000 iterations of parameter selection through Monte Carlo sampling was repeated. Parameter boundaries for each of the alternative cases are presented in Table A-1.

Alternative model 1 (AM1) features an expanded upper boundary of the *Tp* parameter at 100 hours. This relaxed parameter range set delivers predictably improved model performance, recording mean and median NSE scores of ~0.49 and ~0.57, respectively, relative to the selected model (SM), which records mean and median NSE scores of ~0.35 and ~0.52, respectively. Figure A-1 presents AM1 performance across the sample region. For CDFs of optimal calibration model parameters by EH condition, see Figure A-2.

Note that the parameter distributions of *rec_coef, Tp,* and *Ia* separate at the subjectively prescribed levels of statistical significance. Higher values of the *rec_coef* parameter at infested sites indicate that these catchments exhibit shortened groundwater flow pathways, which results agree with the outputs of the SM. CDFs of *Tp* values identify shorter lag times between the beginning of hydrograph rise and hydrograph peak at infested sites, suggesting higher sensitivity of stream discharge responses to precipitation input, likely a result of overland runoff.

Parameter	Boundary Range		
	Selected Model	*Alternative Model 1*	*Alternative Model 2*
forest	(0,1)	(0,1)	(0,1)
Tp (hours)	(0,4)	(0,100)	(0,4)
Ia (mm)	(0.05,0.9)	(0.05,0.9)	(0.05,0.9)
PETmax (mm)	(2,10)	(2,10)	(2,10)
percent impervious	(0,100)	(0,100)	-
rec_coef	(0.0001,0.2)	(0.0001,0.2)	(0.0001,0.2)
C1	(1,5)	(1,5)	(1,5)
Se_{min}	(40,210)	(40,210)	(40,210)

***Table A-1**: JoFlow model parameter ranges for all simulated scenarios.*

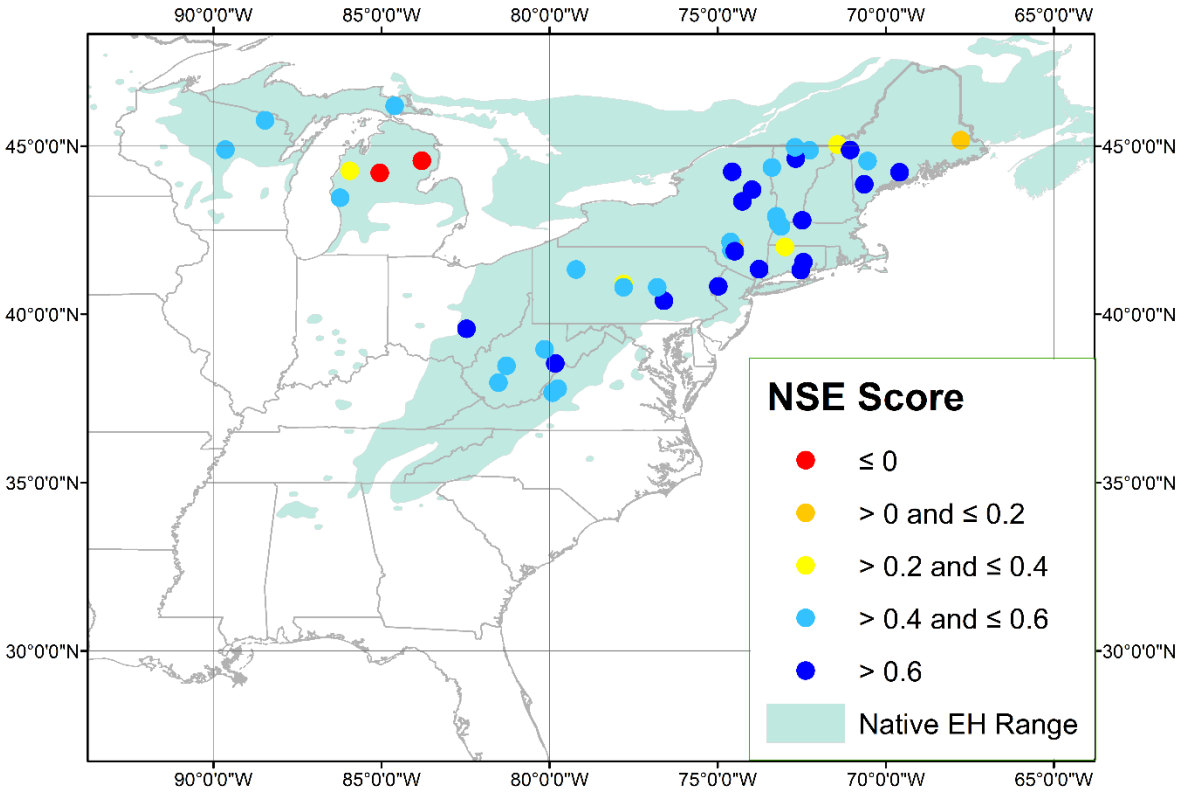

***Figure A-1**: Distribution of site NSE scores for AM1 by geographic location.*

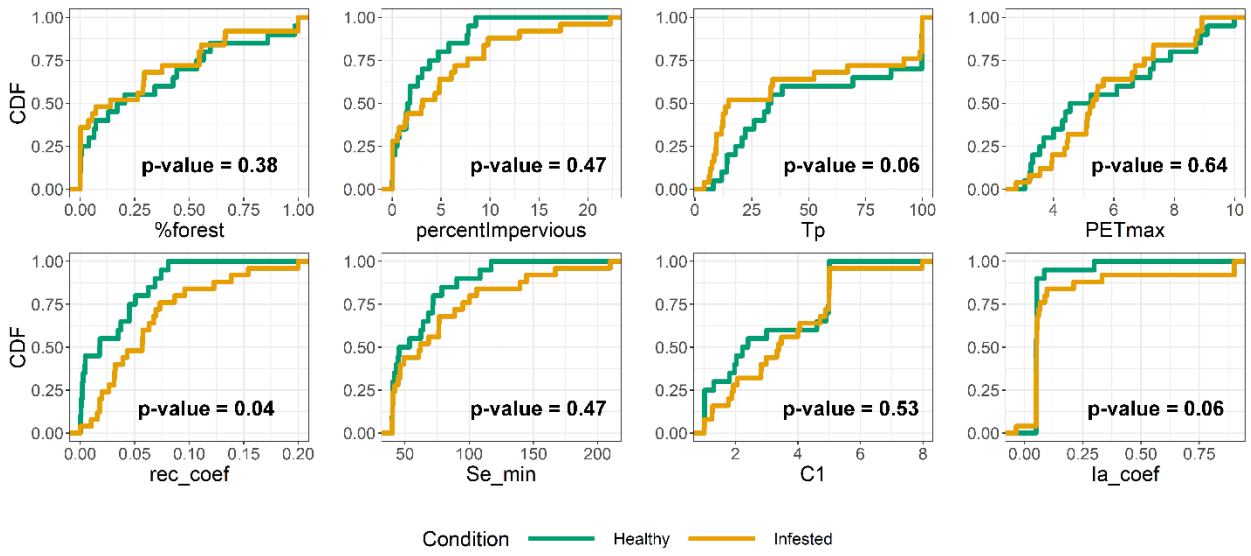

***Figure A-2**: CDF plots of all parameter values by Condition for AM1.*

This result, in concert with the distribution of the *rec_coef* parameter evince that groundwater contributes a greater proportion of total discharge at healthy sites, relative to infested catchments. However, a range of (0,100) for Tp likely lacks physical veracity, the upper boundary for this parameter within the SM is set in accordance with Archibald et al. (2014).

Alternative model 2 (AM2), eliminates the *percent impervious* parameter from calibration. In the supplemental materials to their primary analysis, Knighton et al. (2017a) establish that JoFlow sensitivity to percent impervious is the most critical factor in determining surface runoff, while Se_min and C1 parameters are secondary. The omission of this parameter causes a slight reduction in NSE scores, with mean and median values of ~0.34 and ~0.5, respectively. Figure A-3 presents AM2 performance across all catchments sampled. CDFs of optimal parameter values by EH condition (Figure A-4) illustrate that with the omission of percent impervious, the parameters rec_coef, C1, and Ia exhibit statistically significant separation. These results are also in general agreement with the SM and AM1.

Through multiple modeling approaches with varied parameter considerations but generally convergent outcomes, this study establishes that EH condition influences various hydrologic characteristics, and that HWA infestation may drive the potential for riverine flooding.

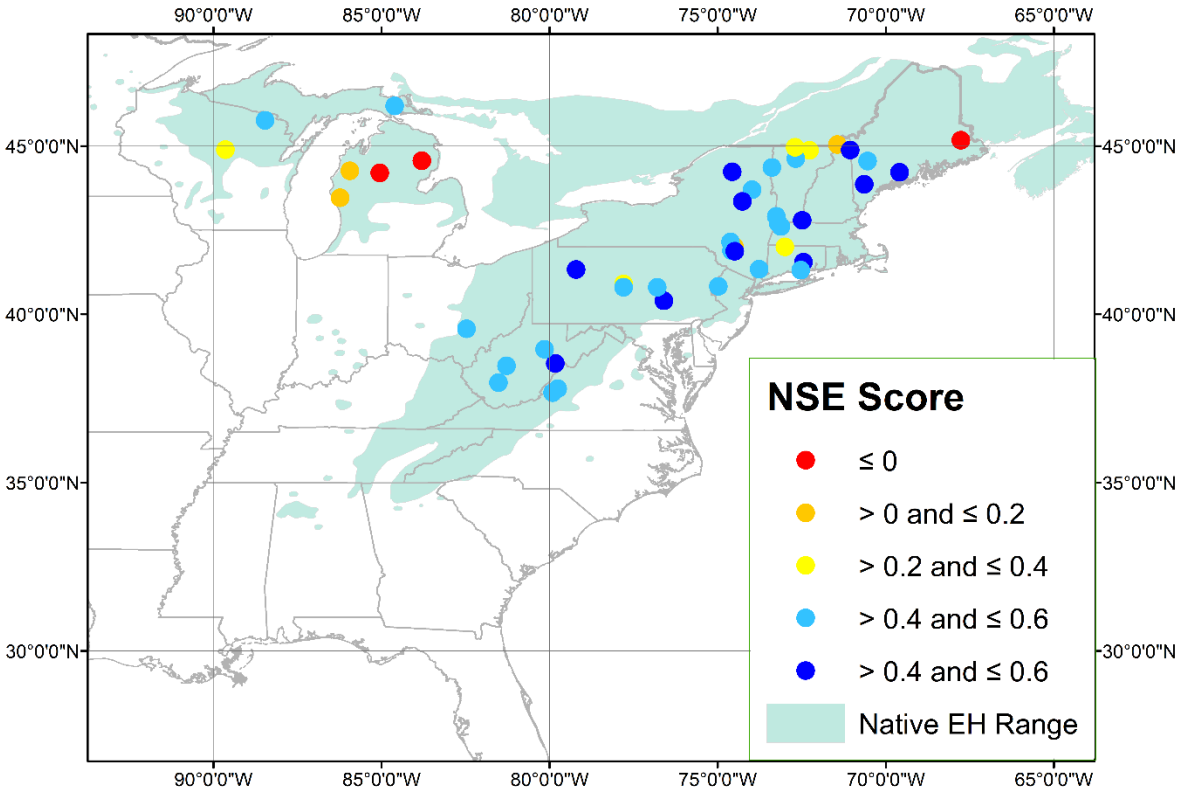

***Figure A-3**: Distribution of site NSE scores for AM2 by geographic location*

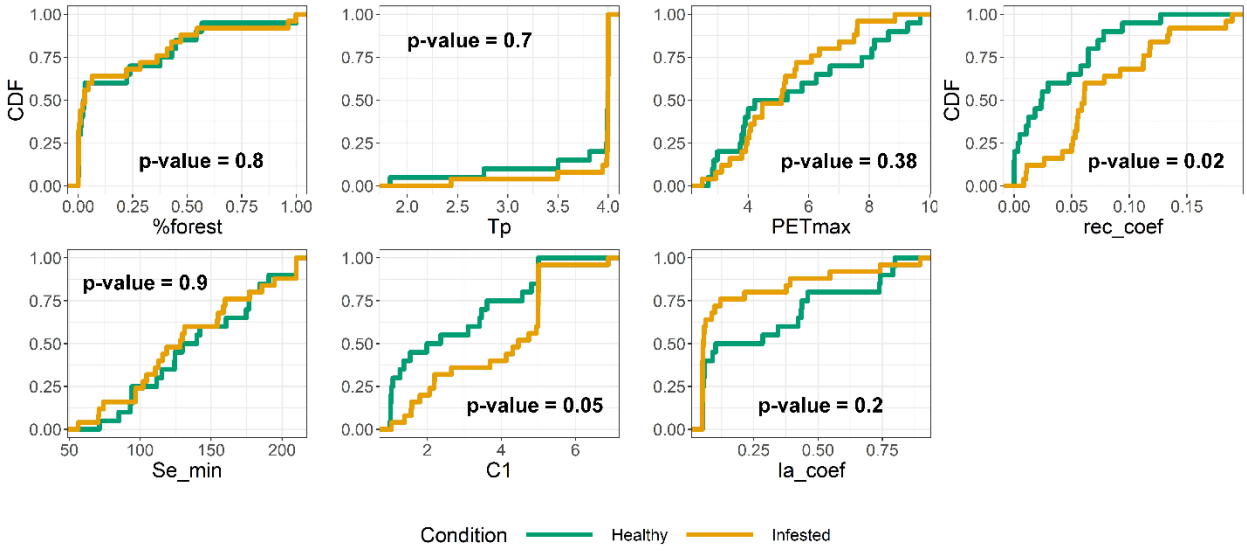

***Figure A-4**: CDF plots of all optimal parameter values by Condition for AM2*